

MÁSTERES de la UAM

Facultad de
Ciencias / 16-17

Física Teórica

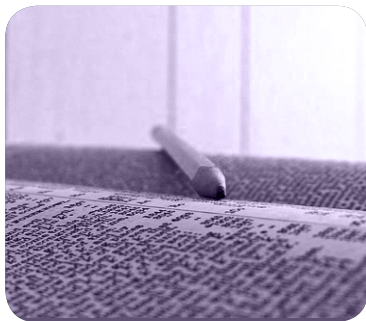


Campus Internacional
excelencia UAM
CSIC+



Numerical Methods in Spin Chains Models

*Héctor Bermúdez
Castro*



Héctor Bermúdez Castro

MSc in Theoretical Physics



Numerical Methods in Spin Chains Models

Dissertation submitted in partial fulfillment of the requirements for the
MSc degree
in
Theoretical Physics

Supervisor : Germán Sierra, Full Professor, CSIC

Thesis Committee:

President: Luca Merlo

Member I: Luis Ibáñez

Member II: Claudia Glasman



Instituto de
Física
Teórica
UAM-CSIC



UNIVERSIDAD AUTÓNOMA
DE MADRID

September, 2017

Numerical Methods in Spin Chains Models

The Facultad de Ciencias and Universidad Autónoma de Madrid institutions have the right, forever and without geographical limitations, to file and publish this dissertation through printed copies reproduced on paper or in digital form, or by any other means known or to be invented, and to disseminate it through scientific repositories and to allow them to be copied and distributed for non-commercial educational or research purposes, provided that the author and publisher are given credit.

A la música. A Marta

Acknowledgements

The author is deeply grateful to his supervisor, Prof. Germán Sierra, for having always such an open and charming smile during the many times he visited him at his office for new doubts and explanations.

All this work presented here would not have been possible as well without the infinite support of so many good friends and colleagues without whom I could not have finished neither this Master's thesis nor the Master's degree itself. For so many good memories playing ping-pong while discussing High-Energy Physics or the tricky human nature, drawing in the blackboard formulae we did not understand, or for just singing in the hard nights of Winter.

None of the programs developed, nor the many problems one has to deal with when using \LaTeX or other programming languages as the ones used here (C++,Python,Mathematica), could have been used and written without the always shadow-hidden help of the mighty Stack Overflow¹ and TeX - Stack Exchange² sites.

And last but not least, none of this would have been possible without many people that deserve a notorious acknowledgement, as friends that will always be remembered. However, special consideration is meant for parents, who without either complete understanding of the motivations or substantial knowledge of the desires and potential future outcomes, always have been the stone over everything could be built. It will never be possible to thank them properly for so much they have given.

¹<https://stackoverflow.com/>

²<https://tex.stackexchange.com/>

Abstract

Quantum spin chain models have been a toy model for exploring more complex theories since first times. In this work, in order to study this particular type of models, numerical methods based on exact diagonalization algorithms are performed. This allows to solve in a direct fashion a quantum many-body problem and to confirm some predictions related to the connection between the lattice discrete Hamiltonian and its continuum field theory limit. One of the most important of these predictions is the statement that there exists a connection between the Heisenberg XXX Hamiltonian and the $SU(2)_{k=1}$ Wess-Zumino-Witten non-linear σ model, which is related to a Conformal Field Theory with central charge $c = 1$. Studies to prove this fact are performed, finding scalings for ground state energies, structure of conformal towers and correlators. A bridge towards Quantum Information ideas is built studying entanglement entropies. Moreover, a connection between the systems studied and the Haldane-Shastry model is explored.

Resumen

Las cadenas cuánticas de espín han sido un sistema físico sobre el que probar teorías más complejas desde los comienzos de la física. En este trabajo, se desarrollarán métodos numéricos basados en algoritmos de diagonalización exacta con el propósito de estudiar este tipo de sistemas físicos. Esto permite resolver directamente un problema cuántico de muchos cuerpos y, a la vez, confirmar predicciones sobre la conexión entre los Hamiltonianos discretos en retículas y sus correspondientes teorías de campos en el límite continuo. De las más importantes de estas predicciones es la existente acerca de la conexión entre el Hamiltoniano isotrópico de Heisenberg y el modelo σ no lineal $SU(2)_{k=1}$ de Wess-Zumino-Witten, que a su vez está relacionado con una teoría conformal de campos de carga central $c = 1$. Varios estudios para probar esta afirmación se han llevado a cabo, hayando cómo las energías de los estados fundamentales escalan, las estructuras de las torres conformes y algunos correladores. Además, se intenta construir un enlace con ideas de información cuántica a través del estudio de entropías de entrelazamiento. También una posible conexión entre los modelos estudiados y el modelo de Haldane-Shastry es explorada.

Contents

1	Introduction	1
2	The Heisenberg spin chain	4
2.1	Models studied	4
2.2	Theoretical framework	6
2.2.1	The Haldane map and the $O(3)$ non-linear σ -models	6
2.2.2	$\theta = \pi$ field theory approaches	8
2.2.3	The $SU(2)_{k=1}$ WZW model	9
2.2.4	CFT with $c = 1$ for the $SU(2)_{k=1}$ WZW model	10
3	Numerical and theoretical methods	13
3.1	Building the Hamiltonian	13
3.1.1	Use of symmetries	15
3.1.2	Additional symmetries	22
3.2	Diagonalization: Krylov space and the Lanczos procedure	24
3.3	Density matrices and tracing over subspaces	25
4	Theoretical predictions and formulae	28
4.1	Finite size scaling	28
4.2	Spectrum and Conformal towers	29
4.3	Correlators and exchange-size dependence	30
4.4	Entanglement entropies and Quantum Information	31
4.5	Haldane-Shastry model and its relation to J_2/J_1 model	33
5	Results and discussion	35
5.1	Finite size scaling	35
5.2	Spectrum and Conformal towers	36

<i>CONTENTS</i>	viii
5.3 Correlators and exchange-size dependence	38
5.4 Entanglement entropies and Quantum Information	39
5.5 Haldane-Shastry model and its relation to J_2/J_1 model	41
6 Conclusions and Outlook	45
Bibliography	46
A Representation theory and CFT explained in detail	51
A.1 Why CFT's are relevant?	51
A.2 Transformations in a CFT and algebras of their generators	53
A.3 Quantum field theories with conformal invariance in a two dimensional theory	55
A.4 Minimal models and highest-weight representation	59
B Programs used and codes	62



Introduction

As great physicist of the epoch soon realized, macroscopic effects in the daily world could be explained paying attention to the microscopic quantum level, as how the interactions between the spins may lead to collective behaviours with macroscopic effects. Particularly, in this work we will refer fundamentally to one of the most studied ones since ancient times: magnetism. In the simplest cases, we can characterize a material as ferromagnetic, where the spins line up parallel to each other, or as anti-ferromagnetic, where neighbouring spins point in opposite directions.

The source of such spontaneous magnetization is the so-called exchange interaction, which has a quantum mechanical origin. It is the manifestation of the Coulomb repulsion between the electrons and the Pauli exclusion principle, being therefore strong and short range (consult [1] and references therein). A magnetic dipolar interaction is also present, but it is too small to explain magnetism at room temperature. The exchange interaction between particles of spin $1/2$ and higher is usually described by the Heisenberg model, as a simplified version of the well-known Ising model [2]. The former, due to its simplicity, has been widely studied and used as a toy model for other theories. Furthermore, physicists have had an analytical solution, with which new results from other approaches could be compared, since 1931, when Bethe derived an exact analytical solution to the one-dimensional spin- $1/2$ Heisenberg model with coupling between nearest-neighbours (NN) [3]. This was a breakthrough in the studies of exactly solvable quantum many-body systems.

Whenever exact solutions of many-body problems like this one, with the interaction of plenty of strongly-correlated particles, was not accessible, the other approach was to reformulate these complicated interacting theories in a way they could become weakly interacting [4, 5]. This was the idea behind the famous 1928's paper by Jordan and Wigner [6] establishing an equivalence between the model of interacting fermions and the anisotropic spin-1/2 Heisenberg model (to which we will refer as the XXZ model), finding a particular case of this model (the XY model) for which the model became non-interacting. However, even out of this particular point, sometimes interactions could be effectively removed by a second transformation, *bosonization*; turning the spin-1/2 Heisenberg model in just a collection of harmonic oscillators. Such transformations hold in the continuum limit whenever the energy is much smaller than the bandwidth.

This type of bosonization, *Abelian bosonization*, coined independently in 1975 by Coleman and Mandelstam and Mattis and Luther [4], showed that correlation functions of Dirac fermions in (1+1)-dimensions could be expressed in terms of correlation functions of free bosonic fields. This solved many problems in a very easy manner, e.g. the Tomonaga-Luttinger case [4].

Afterwards, in 1983/4, *non-Abelian bosonization* was discovered and used by Polyakov and Wiegmann (1983), Witten (1984), Wiegmann (1984), and Knizhnik and Zamolodchikov (1984). It proved to be very useful for problems when spin degrees of freedom were present (consult [2, 4, 5, 7] and references therein).

Those years also witnessed another two important contributions to the low-dimensional physics: the *Haldane's conjecture* about gap in spin systems, and the birth of Conformal Field Theories (CFT) in Condensed Matter Physics.

Almost fifty years later from the Bethe Ansatz, in 1983, Haldane suggested a remarkable difference between one-dimensional anti-ferromagnetic systems of integer and half-integer spins [8–10], namely that the former should be gapped while the latter gapless. This is of significant importance if we remember the necessary condition for a material to be insulating: the existence of an energy gap between the ground state and the first excited states. The importance of this prediction, after its numerical and experimental confirmation together with a rigorous proof [11], was one of the reasons that eventually led the Swedish Academy to the concession of the Nobel Prize in Physics in 2016 to Thouless, Haldane, and Kosterlitz.

Also in 1984, Belavin, Polyakov, and Zamolodchikov, published their famous paper in which a unified approach to all models with gapless linear spectrum

in (1+1)-dimensions was provided [12]. They saw that if an action of a (1+1)-dimensional theory is quantizable (i.e. only linear time-derivatives appear) the linearity of the spectrum guarantees that the system has an infinite dimensional symmetry (conformal symmetry). Using these techniques, researchers like Cardy, Blöte, Nightingale, Dotsenko, and Fateev, found in 1984 [13–16] important connections between finite size scaling and conformal invariance. These results, were put in connection afterwards with the Bethe ansatz by Affleck *et al.* [17].

CFT had been being used in other fields such as Statistical Physics, in which they allowed to obtain the first formulae for entropies, derived by Holzhey, Larsen, and Wilczek [18], who were interested in the study of black holes. However, Vidal *et al.* soon realized those equations could be applied to low-dimensional Physics, more concretely to spin chains [19]. It was one of the first applications of Quantum Information concepts to quantum lattice systems in one dimension, helping to improve our understanding about entanglement at a quantum level in many-body systems like spin chains [20–23].

It is interesting to mention that many distinct numerical algorithms have been used during the years in order to check the predictions of the theories. Although in this work we will follow the route of exact diagonalization and Lanczos methods started back in 1992 [24], nowadays, White’s DMRG algorithms [25, 26] have been the preferred numerical methods to compute and simulate results due to their efficiency and numerical accuracy.

In this work, we will restrict ourselves to the one-dimensional Heisenberg model with periodic boundary conditions (PBC) considering only interactions between nearest-neighbours (NN) and next-to-nearest-neighbours (NNN). We will study and reproduce some of the more important results found since the early beginning of the understanding of the quantum spin chains until nowadays, reaching the realm of Quantum Information. Furthermore, we will deal with specific predictions for the Haldane-Shastry model due to its theoretical interest [27, 28].

This dissertation is distributed as follows. The theoretical framework about general spin- s chains and the path towards it will be summarized in section 2. It will be also in this section that more concrete results about the spin-1/2 case, which will be used throughout the rest of this work and are the main goal of this work, will be presented. Calculations, procedures and results, in sections 3 and 4, and discussion (section 5), will refer hence only to the spin-1/2 case. Finally, conclusions will be derived in section 6.



The Heisenberg spin chain

2.1 Models studied

We consider here the following physical system: a spin chain, which we define as a collection of particles of a given nature, i.e. certain spin, that interact amongst themselves in a given way, which is dictated by a Hamiltonian \mathcal{H} . In order to be more specific, we consider spin chains with L spin- s particles, i.e. with length L . Now, let us use the symbol $S_i^{(m)}$ as the spin operator along direction i for the particle at position m in the chain. Although additional detail is not needed so far, a more practical definition for the operators $S_i^{(m)}$ will be given in equation 3.1 of section 3.1 in terms of tensor products of matrices. For instance, in the case of spin-1/2 particles, they will be related to the traditional σ_i Pauli matrices.

One of the simplest models one could consider when studying spin chains is the usual Heisenberg XXZ model, which is

$$\mathcal{H}_{XXZ} = \sum_{m=0}^{L-1} \{S_x^{(m)} S_x^{(m+1)} + S_y^{(m)} S_y^{(m+1)} + \Delta S_z^{(m)} S_z^{(m+1)}\}, \quad (2.1)$$

where we have assumed $s = 1/2$ and took into account that for a ring (periodic chain) the periodic boundary conditions (PBC) imply that $S_i^{(0)} \equiv S_i^{(L)}$ for all directions, i.e. $i \in \{x, y, z\}$. Note that in this model, the exchange interaction is only considered between nearest neighbours (NN) and a coefficient Δ is added

in order to describe the possible anisotropy of our system. Normally, in the literature this Hamiltonian appears written with a pre-factor J which we are taking equal to unity, which is sometimes called the *clean* Heisenberg model [29]. This is important, since for the whole discussion in this work, $J > 0$ will be taken for granted, in order to describe an anti-ferromagnet. Classically, this kind of magnets has a Néel state as its classical ground state, which can be described as the superposition of two ferromagnetic sub-lattices with magnetization along the same direction but with opposite sense:

$$\begin{array}{cccc} \uparrow & \downarrow & \uparrow & \downarrow \\ \downarrow & \uparrow & \downarrow & \uparrow \\ \uparrow & \downarrow & \uparrow & \downarrow \end{array} .$$

If one forgets about anisotropy (which would lead to the so-called XXX model in the equation above) and extends the interaction to next-to-nearest-neighbours (NNN) one arrives to the J_2/J_1 model

$$\mathcal{H}_{J_2/J_1} = \sum_{m=0}^{L-1} \left\{ \vec{S}_i^{(m)} \vec{S}_i^{(m+1)} + \frac{J_2}{J_1} \left(\vec{S}_i^{(m)} \vec{S}_i^{(m+2)} \right) \right\}, \quad (2.2)$$

with $\vec{S}^{(i)} = (S_x^{(i)}, S_y^{(i)}, S_z^{(i)})$. Here, the ratio J_2/J_1 describes the importance of the interaction between NNN with respect to NN. This model has the important property that is critical for a value of $J_2/J_1 \approx 0.2411$, since it is a fixed point Hamiltonian under renormalization flow (its β -function vanishes). As previously in the XXZ model, we have assumed that $J_1 = 1$, but still keep writing J_2/J_1 to make it easier for the reader to consult bibliography.

These models, and all their variants (namely, different points in the Δ and J_2/J_1 spaces), may be easily visualized in a map or phase-diagram.

Firstly, we can characterize different systems according to the value of the anisotropy parameter Δ in equation 2.1. Some interesting points are the *free-fermion point* ($\Delta = 0$) and the *isotropic point* ($\Delta = 1$). For $\Delta > 1$, a spin gap opens and the system enters an anti-ferromagnetic Ising phase; otherwise, for $\Delta < -1$, the chain becomes a gapped Ising ferromagnet. The region with $\Delta \in (-1, 1]$ is critical, and in the isotropic point, it is SU(2) invariant, which means that the Hamiltonian \mathcal{H} commutes with the total spin operator \vec{S} defined as

$$\vec{S} \equiv \sum_{m=0}^{L-1} \vec{S}^{(m)}. \quad (2.3)$$

Moving up in length of interaction and reaching the isotropical J_2/J_1 model of equation 2.2, there is a magnetically disordered spin-rotation-invariant quantum phase in the region of strong frustration $0.44 \lesssim J_2/J_1 \lesssim 0.6$. Although the semi-classical ground state phases of the model, namely the Néel Anti-Ferromagnetic long-range order (NAF LRO) at $J_2/J_1 \lesssim 0.44$ and the Collinear Anti-ferromagnetic (CAF) LRO at $J_2/J_1 \gtrsim 0.66$ are well-understood, very recent calculations using Density Matrix Renormalization Group (DMRG) with explicit implementation of SU(2) spin-rotation symmetry have found a gapless spin liquid for $0.44 < J_2/J_1 < 0.5$ and a gapped plaquette valence bond phase for $0.5 < J_2/J_1 < 0.61$, as is explained in [30] and references therein.

2.2 Theoretical framework

2.2.1 The Haldane map and the $O(3)$ non-linear σ -models

It is easy to see that the quantum ground state for a Heisenberg XXZ model of equation 2.1 is not the classical Néel state if one notices first that each spin operators pair can be rewritten as

$$\frac{1}{2} \left(S_+^{(m)} S_-^{(n)} + S_-^{(m)} S_+^{(n)} \right) + S_z^{(m)} S_z^{(n)}, \quad (2.4)$$

which allows us to separate very clearly the diagonal $S_z^{(m)} S_z^{(n)}$ from the off-diagonal ones. Note that the traditional definition of the raising/lowering operator was used, namely $S_{\pm}^{(m)} \equiv S_x^{(m)} \pm iS_y^{(m)}$.

If one perturbs away from a limit in which the Néel state becomes exact, as occurs for the spin- s Heisenberg anti-ferromagnet when $s \rightarrow \infty$, one finds that the Néel state is destabilized by quantum fluctuations in one dimension, no matter how large the spin s is. This is due to the fact that the spin representation used, in terms of boson operators which eventually will describe spin-waves, shows that excitations correspond to infinitesimal deviations of the spins away from the Néel state. The two boson operators, which are Goldstone modes corresponding to the breaking of $SO(3)$ down to $SO(2)$, are connected to infra-red divergences and are precisely the cause why the destabilization occurs. Thus, we cannot take the Néel order for granted, even for the pure nearest neighbour Heisenberg XXZ model, at $s = 1/2$.

The interest in developing a low-energy continuum limit of quantum anti-ferromagnets is which led Haldane to derive the so-called *Haldane's map* between

the \mathcal{H}_{XXX} Hamiltonian and the $O(3)$ non-linear σ -model:

$$\mathcal{H}_{O(3)\text{-nl}\sigma\text{m}} = \frac{v}{2} \left\{ g^2 \left(\vec{l} - \frac{\theta}{4\pi} \vec{\varphi}' \right)^2 + \frac{\vec{\varphi}'^2}{g^2} \right\}, \quad (2.5)$$

with velocity, coupling constant, and *topological angle*:

$$v = 2Js, \quad g = 2/s, \quad \theta = 2\pi s.$$

The Haldane's map is obtained after "integrating-out" the high-energy modes, keeping just the Fourier modes of $\vec{S}^{(m)}$ near the problematic wave vectors, as $\vec{k} = 0$, and assuming

$$\vec{S}^{(m)} \approx s\vec{\varphi}^{(m)} + \vec{l}^{(m)}, \quad (2.6)$$

where $\vec{\varphi}$ and \vec{l} are fields that vary slowly on the lattice scale. This allows one to use a gradient expansion ($\vec{\varphi}'$) to obtain equation 2.5 after making the arbitrary choice of combining each spin on an even site (at $2m$) with the spin to its right ($2m + 1$).

It can be seen that the $\mathcal{H}_{O(3)\text{-nl}\sigma\text{m}}$ Hamiltonian follows from the Lagrangian:

$$\mathcal{L}_{O(3)\text{-nl}\sigma\text{m}} = \frac{1}{2g} \partial_\mu \vec{\varphi} \partial^\mu \vec{\varphi} + \frac{\theta}{8\pi} \epsilon^{\mu\nu} \vec{\varphi} \cdot (\partial_\mu \vec{\varphi} \times \partial_\nu \vec{\varphi}), \quad (2.7)$$

with $\vec{\varphi}^2 = 1$, being hence a vector in a two dimensional sphere \mathcal{S}_2 with unitary radius. We now see that the term proportional to the topological angle θ is a total derivative, whose integral (which appears in the action) measures the winding number of the map from the sphere onto the sphere. If we denote the (integer) integral by Q to keep in mind its origin as a *topological charge*, we can write the action as

$$\mathcal{S}_{O(3)\text{-nl}\sigma\text{m}} = \mathcal{S}_0 + i\theta Q. \quad (2.8)$$

Since $\theta = 2\pi s$, we will have $\theta = 0$ or $\theta = \pi$ for spin s an integer or a half-odd-integer respectively, which allows us to see that we will always have parity conservation in the continuum limit. It took some years to completely understand what this separation in spin sectors led to, eventually finding that terms with $\theta = 0$ (π) describe gapped (gapless) systems and map to different field theories. The non-linear σ -model with $\theta = 0$ was solved by Polyakov, who showed that the model was asymptotically free and a gap was generated dynamically in the spectrum. This was the result that Haldane used to predict that whenever the spin s was an integer, the Heisenberg Hamiltonian would have a gap

in the spectrum. This is, among many others, another example of the intimate connection between High Energy Physics and Condensed Matter.

2.2.2 $\theta = \pi$ field theory approaches

Although the XXX Heisenberg model for spin-1/2 particles had been already solved analytically in 1931 by Bethe as said in section 1, and the XXZ model was solved by Yang and Yang in 1966 [31–33], it was not yet understood how field theories could apply to them.

One approach, followed by Affleck [34] and only valid for $s = 1/2$, was based on using Jordan-Wigner transformations, to represent spin operators as *spinless* fermions ψ via

$$S_+^{(m)} = \psi^{(m)} \exp \left[i\pi \sum_{l=0}^{m-1} (\psi^{(l)})^\dagger \psi^{(l)} \right], \quad (2.9)$$

to the free-fermion point of the XXZ Heisenberg model ($\Delta = 0$ in equation 2.1) and perturb the system away in order to obtain the anti-ferromagnetic case ($\Delta = 1$). He found that his Hamiltonian described a Lorentz-invariant massless Dirac fermion field theory in the low-energy approximation. It contained an interaction term with chiral currents $J_{L,R}$, whose Lagrangian was exactly the one of the *Thirring model*:

$$\mathcal{L}_{\text{Thirring}} = -i \left(\psi_L^\dagger \partial_- \psi_L + \psi_R^\dagger \partial_+ \psi_R \right) - 4\Delta J_L J_R, \quad (2.10)$$

solvable by bosonization.

His results were verified afterwards by a more general approach followed by Affleck and Haldane [9], in which they use a generalized *Hubbard model* representation with Hamiltonian

$$\mathcal{H}_{\text{Hubbard}} = \sum_{n \neq m} \left(\psi^{(m)\dagger \alpha} \psi^{(n)}_{\alpha} + \text{h.c.} \right) - U \sum_m \vec{S}^{(m)} \cdot \vec{S}^{(m)}, \quad (2.11)$$

where

$$\vec{S}^{(m)} = \frac{1}{2} \psi^{(m)\dagger \alpha} \sigma_{\alpha}^{\beta} \psi^{(m)}_{\beta}, \quad (2.12)$$

and t is the probability for transitions between neighbouring atoms for electrons in well-localized atomic orbitals, and U represents a highly screened Coulomb repulsion between electrons.

Their goal was to use non-Abelian bosonization to argue that the critical theory for generic half-odd-integer spin anti-ferromagnets (as the XXZ and J_2/J_1 models described in the previous section of this chapter) is the *Wess-Zumino-Witten* model with *topological coupling* k .

2.2.3 The $SU(2)_{k=1}$ WZW model

After the non-Abelian bosonization of the model of equation 2.11, they found [9, 34] that the free-fermion theory (i.e. $U = 0$), which has charge $U(1)$ ($\psi_{L,Ri\alpha} \rightarrow e^{i\theta}\psi_{L,Ri\alpha}$) and spin $SU(2)$ ($\psi_{L,Ri\alpha} \rightarrow g_{\alpha}^{\beta}\psi_{L,Ri\beta}$) symmetries, was equivalent to decoupled theories for the fields φ and g :

$$\mathcal{L}_{WZW}(\varphi) = \frac{1}{2}\partial_{\mu}\varphi\partial^{\mu}\varphi, \quad (2.13)$$

$$\mathcal{S}_{WZW}(g) = \frac{1}{8\pi} \int d^2x \text{Tr} \partial_{\mu} g^{\dagger} \partial^{\mu} g + \frac{k}{12\pi} \int d^3x \epsilon^{\mu\nu\lambda} \text{Tr} g^{\dagger} \partial_{\mu} g g^{\dagger} \partial_{\nu} g g^{\dagger} \partial_{\lambda} g, \quad (2.14)$$

where g is the WZW matrix representing the $SU(2)$ degrees of freedom and $\varphi(x)$ is a single scalar field representing the $U(1)$ degrees of freedom. Models with $U \neq 0$ were found to flow to the $U = 0$ case under renormalization.

One can also study a generalized Hubbard model representation for the spin chain in which a strong Hund's rule coupling between the electrons at different orbitals in each atom of the chain was added. We will refer to the orbital index as the *color*, whose number n_c satisfies that $n_c = 2s$, so in our case $n_c = 1$. They found that the topological coupling of the WZW models fulfilled $k = n_c$ and they finally proved that this was the low energy theory for a large total spin- s chain described by a $O(3)$ non-linear σ -model at the topological point $\theta = \pi$.

Also, the $k = 1$ WZW model represents a stable fixed point for many $SU(2)$ invariant systems due to a type of topological stability. In particular, the Bethe ansatz integrable spin- s Hamiltonian is attracted to the $k = 2s$ multicritical point [17].

The energy-momentum tensor T_{WZW} of this model can be written in a form quadratic in the currents J and it is chiral¹, i.e. we have a chiral $SU_L(n_c) \times SU_R(n_c)$ symmetry in our system. The expression for its left or chiral part T_L is given by

$$T_L = \frac{\pi}{2n_c} v J_L J_L + \left(\frac{2\pi}{n_c + 2} \right) v \vec{J}_L \cdot \vec{J}_L + \left(\frac{2\pi}{n_c + 2} \right) v J_L^A J_L^A, \quad (2.15)$$

with v the velocity of light and A being the color index. Its structure suggests that the theory can be separated into charge $U(1)$, spin $SU(2)$, and color $SU(n_c)$ sectors. Constructing the chiral part of the energy-momentum tensor using the currents of the field theory is called the *Sugawara construction*, which is inspired in the algebra followed by the currents in the field theory².

¹Consult section A.3 for more details.

²Consult equations A.43, A.44 and A.45 and the explanations of section A.3.

However, up to this point, no mention to the reason why these models should occur as the critical theories has been given. The answer is perfectly given in the lecture given at *Les Houches* in 1988 by Affleck [34]:

This can be understood by realizing that any theory invariant under parity (which generally holds for lattice models as the ones considered in this work) and a continuous symmetry group G , will necessarily have a chiral symmetry group (usually $G_L \times G_R$) at any possible critical point. The reason is simply that only chiral symmetries are compatible with conformal invariance.

Note how perfectly the requirements are fulfilled as it is explained in the paragraph just before the quotation. The fact that critical points under renormalization accept a description by a CFT is due to its lack of scale, since in a critical point long-range order and correlations occur in the physical system. Being able to describe our system by CFT's allows us to find the critical exponents for finite size scalings and expressions for the correlators in a more direct way. This shows the perfect 1-to-1 correspondence between the CFT and the QFT, in which a particular state of a representation of the algebra corresponds to a field.

2.2.4 CFT with $c = 1$ for the $SU(2)_{k=1}$ WZW model

Considering commutation relations obeyed by the currents appearing in T_L , defined in equation 2.15, we find that the $SU(2)$ currents obey a *Kac-Moody algebra*³ with *central charge* $k = n_c$, which is also the algebra obeyed by the currents in the WZW model with topological coupling constant k , which appears in the action of equation 2.14.

Before going any further, the reader without familiarity with the general features of CFT's is encouraged to read the appendix A for a brief introduction, coming back here to this point afterwards⁴.

The WZW model with topological coupling constant k represents the minimal conformal theory for a given value of k in the sense that, given any conformal invariant theory with $SU(2)$ currents obeying a Kac-Moody algebra with central charge k , we may define an energy-momentum tensor T quadratic in currents as the one that appears in equation 2.15. This tensor is not necessarily the full energy-momentum tensor of the theory, because, although it does generate the

³Consult equation A.20 in appendix A for the definition of a *Kac-Moody algebra*.

⁴Hereinafter, all the new concepts that are explained in the appendix A are written in italic formatting, and will not be explained in this section.

spatial and time translations of the currents, a full and more general T could still be defined adding to the actual part a new term that commutes with all the currents, i.e. $[T_L, T_L^{(\text{new})}] = [T_L^{(\text{new})}, \vec{J}_L] = 0$. This explains why, in order to obtain the smallest possible conformal anomaly parameter c (and hence fewest massless particles and a more dominant long-range interaction) of the equivalent CFT, this additional contribution $T_L^{(\text{new})}$ must be null, since the total c will be the sum of that for T_L , and that for $T_L^{(\text{new})}$.

A complete classification of *primary fields* and of the spectrum has been performed for the WZW models [35]. It was found that there exists one operator with *scaling dimension* x , which can be written in terms of the spin of the operators that must have specific values, namely $s_L = s_R = 0, \frac{1}{2}, \dots, \frac{k}{2}$. The expression for x is as follows:

$$x = 2 \frac{s_L(s_L + 1)}{2 + k}. \quad (2.16)$$

In our case of interest, $n_c = k = 1$, only non-relevant operators are permitted, since $s_L = 0$ is the identity $\mathbb{1}$ and $s_L = \frac{1}{2}$ is the energy-momentum tensor of the system, with dimension (for $k = 1$) $x = 1/4$. While the former correspond to states with momentum near 0, the latter has momentum close to π , given the parity of the operators.

We can use the chiral and anti-chiral components of the energy-momentum tensor T constructed with the currents, namely T_L and T_R , to define the momentum \mathcal{P} and Hamiltonian \mathcal{H} operators:

$$\mathcal{P} = T_L - T_R, \quad (2.17)$$

$$\mathcal{H} = v(T_L + T_R), \quad (2.18)$$

with v being the velocity of light, which for the XXX Heisenberg model is equal to $\pi/2$.

Since the *raising operators* are in general the Laurent modes of the energy-momentum tensor T , in CFT's with conserved currents we can also use as raising operators the Laurent modes of the currents. Using this fact and the relations derived from the Kac-Moody algebra for the $SU(2)_{k=1}$ WZW model, it can be proven [17] that two distinct *conformal towers* (for momentum $P = 0$ and for $P = \pi$) emerge, as will be explained in sections 4.2 and 4.1 and seen in the corresponding results of section 5.2.

Due to the Sugawara construction of the energy-momentum tensor in the field

theory, the central charge of the CFT is given by the following equivalent expressions

$$c = \frac{k \dim(G)}{c_\nu + k}, \quad (2.19)$$

$$c = \frac{\pi}{4} \frac{J^a J^a}{(c_\nu + k)}, \quad (2.20)$$

with $G = SU(2)$ (and hence $\dim(G) = 3$) and c_ν being a quadratic Casimir operator in the adjoint representation satisfying

$$c_\nu \delta^{cd} = \sum_{a,b} f^{abc} f^{abd}, \quad (2.21)$$

with f^{abc} being the structure constants of the symmetry group (in our case ϵ^{abc}). The equivalence between equations 2.19 and 2.20 can be proven using equations A.18 and A.19 of section A.2. It is easy to show also that, given the structure constants of the $SU(2)$ group, $c_\nu = 2$, yielding the formula appearing in [17]

$$c = \frac{3k}{2 + k}, \quad (2.22)$$

which equals 1 when $k = 1$. It is interesting to remark that, in order to have an unitary representation of the Kac-Moody algebra, we must have $k > 0$ (which yields $c \geq 1$) [36].



Numerical and theoretical methods

In order to study numerically any of the systems discussed so far, we need their Hamiltonians \mathcal{H} , whose generation and diagonalization has not been mentioned yet. It will be explained in sections 3.1 and 3.2. Although many fast and powerful algorithms have been developed until today (e.g. the outstanding results obtained by DMRG [37]) in this work we take a more humble path: exact diagonalization. It is a route which, although constrains us to sizes relatively small, allows us to obtain the full spectrum without having to be worried about approximations or assumptions as low-entanglement-entropy, etc. These DMRG algorithms led afterwards to what nowadays are called *Tensor Networks*, being the DMRG the first example of a particular subclass, the *Matrix Product States* or MPS. Their generalization to two dimensional models are the *Projected Entangled-Pair States* or PEPS, and were firstly proposed by Verstraete and Cirac [38–40].

Furthermore, apart from the construction of the Hamiltonian matrix and its diagonalization, it is also important to explain the completely original algorithm (according to the author’s knowledge) used in the construction of the reduced density matrices (section 3.3) to trace over subspaces.

3.1 Building the Hamiltonian

When we defined the XXZ and the J_2/J_1 models in equations 2.1 and 2.2 of section 2.1, we used the symbol $S_i^{(m)}$ to describe the spin operator along direction

i for the s -spin particle at position m in the chain without giving any further information.

If, as in the rest of this work, one takes $s = \frac{1}{2}$, one possible description is to use the mapping $|\downarrow\rangle \rightarrow \begin{pmatrix} 1 \\ 0 \end{pmatrix}$ and $|\uparrow\rangle \rightarrow \begin{pmatrix} 0 \\ 1 \end{pmatrix}$ in order to describe these operators in a matrix fashion:

$$S_i^{(m)} \equiv \frac{1}{2} \overbrace{\mathbb{1}_{2 \times 2} \otimes \dots \otimes \mathbb{1}_{2 \times 2}}^m \otimes \sigma_i \otimes \overbrace{\mathbb{1}_{2 \times 2} \otimes \dots \otimes \mathbb{1}_{2 \times 2}}^{L-m-1}. \quad (3.1)$$

Note that due to the fast exponential growth of the size of the Hilbert space for a chain of L sites (2^L) this definition is only formally useful, given that in order to obtain the spectrum of the Hamiltonian, one would have to diagonalize a 2^L sparse hermitian square matrix. Instead, it is more convenient, and consumes less resources, to look at the action of the Hamiltonian on a particular state using the alternative equivalent description of equation 2.4.

While the diagonal term ($S_z^{(m)} S_z^{(n)}$) leaves invariant a pair of spins adding just a positive (negative) $\frac{1}{4}$ prefactor for parallel (anti-parallel) spins, the off-diagonal terms (the rest) only act yielding non-null result for anti-parallel spins, exchanging the spins and adding a positive $\frac{1}{2}$ prefactor. We can use this to simplify a lot the construction of the Hamiltonian by iteration over the distinct states conforming the basis instead of Kronecker-multiplying very large and sparse matrices, although its size has not been yet reduced.

However, we have not yet used symmetries. Before doing so, let us define a following suitable notation for the basis: $|0\rangle_b \equiv |\downarrow\rangle$ and $|1\rangle_b \equiv |\uparrow\rangle$. This trivially defines the translation of a particular state of the chain into a binary basis. Take, e.g. $L = 3$ and the state $|\downarrow\uparrow\downarrow\rangle$. With this new notation it would be written as $|010\rangle_b \equiv |2\rangle$, with $|010\rangle_b \equiv |0\rangle_b \otimes |1\rangle_b \otimes |0\rangle_b = (01000000)^T$. We used the subscript $_b$ to refer to the binary basis only.

It is important to note that the treatment and discussion summarized here correspond to the one discussed in the exceptional book by Sandvik [41] about the many subtleties around the Heisenberg spin chain. Together with the explanations, a pseudo-code to guide them will added. If one is instead interested about the actual implementation used by the author in C++ language, the reader is encouraged to take a look at the code, included in appendix B.

3.1.1 Use of symmetries

The fact that the Hamiltonian of the J_2/J_1 model contains terms of the form of equation 2.4 which are $SU(2)$ invariant (together with additional symmetries) means that there exist a set of operators \hat{O} that commutes with the Hamiltonian \mathcal{H} and allow us to define a common basis and write the Hamiltonian as a block-diagonal one.

3.1.1.1 Fixed total S_z sector

We can start choosing a small but very powerful symmetry, the conservation of the magnetization M , i.e. conservation of the total spin of a given state along one particular direction:

$$M \equiv \sum_{m=0}^{L-1} S_z^{(m)}. \quad (3.2)$$

Note that above, without loss of generality, we chose the z -direction to define the magnetization, as it is usually done. This symmetry physically means that, after acting with a Hamiltonian \mathcal{H} made up of terms of the form of equation 2.4 over a particular state $|s\rangle$ (using the notation aforementioned), the number of spins up and down does not change.

This clearly shows that the first step to reduce the size of the Hamiltonian matrix is to determine which of all the states conforming the natural basis of a chain of length L , i.e. $|x\rangle$ with $x \in [0, 2^{L-1}]$, are in the block of fixed magnetization M , which can take values between $[-L/2, -L/2 + 1, \dots, L/2]$.

It can be easily carried out by the following pseudo-code:

```

1   for x in (0, ..., 2^(L-1)):
2       state = binary(x, L)
3       counter = 0
4       for i in (0, ..., L-1):
5           if state[i] = 1:
6               counter++
7               if counter = M + L/2:
8                   add x to basis
9   sort basis

```

Firstly, we use the function `binary(s, L)` to create a binary array `state` of length `L` whose bits form the binary representation of the number `s`. For instance, `binary(3, 5) = [0, 0, 0, 1, 1]`. Then, we simply iterate over its elements

and count the number of ones we find (i.e. spins up). Checking each entry of the binary array can be understood via

$$\text{state}[i] = \langle x | \left(S_z^{(i)} + \frac{1}{2} \right) | x \rangle. \quad (3.3)$$

After counting them, if the number satisfies the condition to belong to the selected fixed magnetization sector (this condition comes from the fact that both $M = \frac{1}{2}(n_\uparrow - n_\downarrow)$ and $L = n_\uparrow + n_\downarrow$ hold) we store this number in the `basis` list, which will contain the whole basis. Finally, we sort the elements of the basis from smaller to higher with the function `sort basis`. Hence, our reduced Hamiltonian with fixed magnetization \mathcal{H}_M will be a square matrix of dimension equal to the length of the basis set. For example, for $(L, M) = (4, 0)$ the basis would be $(3, 5, 6, 9, 10, 12)$ and the Hamiltonian \mathcal{H}_M will have $6 \times 6 = 36$ entries, instead of $2^{2 \times 4} = 256$, which is an important reduction.

Once the basis is computed, we generate the Hamiltonian matrix entries by acting over each element of the basis in the following manner:

```

1   for i in (0, ..., length(basis)-1):
2       state = binary(s[i], L)
3       for ii in (0, ..., L-1):
4           if state[ii] = state[ii+1 mod L]:
5               H[i, i] += 1/4
6           else:
7               H[i, i] -= 1/4
8               state' = flip(state, ii, ii+1 mod L)
9               j = index(state', basis)
10              if j >= 0:
11                  H[i, j] += 1/2

```

where we have already taken into account the way an operator of the form of equation 2.4 acts over a particular state as mentioned previously. The program goes through the elements of the basis, generating a binary array `state` for each element via the function `binary` as before, and starts checking whether or not the bits `ii` and `ii+1 mod L` are equal. Note here how the nature of the PBC present in our model emerges, since we consider the bit `ii+1 mod L` instead `ii+1`.

In the first case scenario, when the bits are equal, only the diagonal part,

$S_z^{(m)} S_z^{(n)}$, acts, while in the other case both parts play their role. While the diagonal does not change the vector, the off-diagonal term $S_+^{(m)} S_-^{(n)} + \dots$ flips the bits, turning the bit ii into $ii+1 \bmod L$ and viceversa generating thus a new binary array `state'`.

Finally, we check which state this new array represents, searching in the basis via the function `index(state', basis)`. This function retrieves the position j of the state represented by `state'` in the set `basis`, which allows us to fill the entry $[i, j]$ of the Hamiltonian. In the case this state is not in the base, it returns -1 , which explains the `if` statement in line 10 of the pseudo-code. For instance, if our basis is made up of the states $\{|3\rangle, |6\rangle, |9\rangle, |12\rangle\}$, represented by the already sorted array `basis=[3, 6, 9, 12]`, then `index(6, basis)=1`. One can also understand this `index` function as the inverse of retrieving one element from the basis array, since the following is fulfilled: if `basis[a]=state` then `index(state, basis)=a`.

Note that in this example we only consider NN interaction. In order to go beyond, one would just have to add a new `for` loop that iterates over the values of the interactions (for instance, 1 and 2 for NN and NNN as in the J_2/J_1 models) modifying the contributions to the entries if anisotropies or different couplings were to be considered.

Furthermore, since our Hamiltonian matrix is hermitian (actually, real and symmetric) we could just store the elements above the diagonal, which will make faster the procedure and will make lower the memory requirements. This is in fact what has been done in the actual code.

However, for a ring of e.g. 12 spins, the Magnetization = 0 sector, in which our ground state lives, is still of dimension $\binom{12}{6} = 924$. This, although not too big, could slow us a lot if many different models had to be computed and necessary diagonalizations procedure had to be carried out. To move down in the size of the Hamiltonian, we can use additional symmetries, as it is explained next.

3.1.1.2 Fixed momentum P sector

Thanks to our periodic boundary conditions (PBC), any state of the ones conforming the basis with fixed Magnetization will be invariant under the Translation operator T . This operator, when acting over a particular state $|s\rangle$ exchanges each one of the spins with his right-neighbour (it may have also been defined with the left-neighbour). For instance, in a chain of 4 spins: $T|5\rangle = T|0101\rangle_b = |1010\rangle_b = |10\rangle$. Obviously, we have that $T^L = \mathbb{1}$ by PBC. However, note that depending on the state considered, we may need a power less than L to leave a particular

state invariant under the consecutive action of T . To continue with the previous example: $T^2|5\rangle = T|10\rangle = |5\rangle$. Since, by rotation of the chain using the translation operator T and keeping in mind PBC both states $|5\rangle$ and $|10\rangle$ are related, we may think that they form a particular set closed under the action of T . For example, this means that we will never be able of getting the state $|3\rangle$ acting over $|5\rangle$ with any power of T , i.e. they fell into different classes.

Thus, whenever a closed set under the action of T is found, we may define a new state as a linear combination of the elements of this closed set. This new state, after properly-fixing the coefficients in the linear combination, will be invariant under T , which means that total momentum P of this state will be conserved. Given that our Hamiltonian \mathcal{H}_{J_2/J_1} , defined in equation 2.2, commutes with T , we can find a common basis of momentum states $|\Psi(P)\rangle$ such that

$$T|\Psi(P)\rangle = e^{iP}|\Psi(P)\rangle. \quad (3.4)$$

Here, the allowed momenta are $P = \frac{2\pi n}{L}$, with $n = 0, \dots, L-1$, following from the fact that $T^L = \mathbb{1}$. In order to construct this new basis $\{|\Psi(P)\rangle\}$ with momentum P well defined, we will use each of these classes closed under the action of T as we illustrated before. Since any of the states of a class can be reached using T from any other belonging to the same class, it seems reasonable to only store the smallest integer state $|a\rangle$ as its *representative*, and construct the rest by using T . This can be done implementing the following pseudo-code:

```

1   for state in basis_with_fixed_M:
2       if state is not in any class yet:
3           create new class
4               add state to the class
5               state' = T(state)
6               multiplicity = 1
7               while state' != state:
8                   add state' to the class
9                   multiplicity++
10                  state' = T(state')
11                 representative = min(class)

```

We start by iterating over all the states `state` inside the already built basis with fixed value of the Magnetization `basis_with_fixed_M`. If the state considered is not in any class yet (initially there is no class constructed), we create a new

class adding the state to it. Then, we act with the translation operator over the state and form a new state `state'` by the function `T(state)` and initialize its `multiplicity` to 1. By repeating this procedure acting more times with T over the states generated until we reach the initial one, we can generate a whole class closed under T with its multiplicity. This multiplicity will be the minimum power of T we have to use to leave a particular state $|x\rangle$ invariant, and all the states inside the same class will have the same multiplicity. Finally, once the whole class is generated, we only store the minimum integer a of the class as its representative, which we will refer to as the state $|a\rangle$.

Having all the representatives of the different classes inside a fixed Magnetization sector of our Hilbert space, we can now generate the basis of well-defined momentum via the equation [41]:

$$|\Psi(P)\rangle = \frac{1}{\sqrt{N_a}} \sum_{r=0}^{L-1} e^{-iPr} T^r |a\rangle, \quad (3.5)$$

which clearly satisfies (as it should) the condition of equation 3.4 that defines the action of the operator T . The constant N_a is a normalization constant that takes care of the fact that states belonging to different classes may have different multiplicities and appear more than once in the sum, and its value is given by:

$$N_a = \frac{L^2}{R_a}, \quad (3.6)$$

where R_a is the multiplicity of the representative state $|a\rangle$. Note that, if $R_a = L$, i.e. we have to use T^L to go from the representative to itself, $N_a = L$, as it should, and each state $T^r |a\rangle$ only appears once in the sum. Besides, it is important to note that not all momenta are compatible with a given representative and hence not allowed, since they must fulfil

$$P = \frac{2\pi}{R_a} m, \quad m = 0, 1, \dots, R_a - 1. \quad (3.7)$$

After all this, we can construct our basis of well-defined momentum via:

```

1   for a in set_of_representatives:
2       condition = check(a,P)
3       if condition:
4           create new P_state
5           P_state = sqrt(multiplicity(a))/L * ...
6               sum(exp(-IPr) * T^r(a), r in (0, ..., L-1))

```

```
7 | add P_state to basis_with_fixed_P&M
```

We iterate over the set of representatives computed before and check whether each a is allowed by the momentum P chosen, using the function `check(a, P)`, that returns a boolean variable `true` or `false`. When the representative is allowed and the condition is fulfilled, we create a new momentum state `P_state` and add it to the basis `basis_with_fixed_P&M`.

Finally, now that our well-defined momentum basis is created, it is time to construct the Hamiltonian. We can split the pair-terms appearing in our Hamiltonians as suggested by equation 2.4:

$$\mathcal{H}_0 = \sum_{n=0}^{L-1} S_z^{(n)} S_z^{(n+1)}, \quad (3.8)$$

$$\mathcal{H}_m = \frac{1}{2} \left(S_+^{(m)} S_-^{(m+1)} + S_-^{(m)} S_+^{(m+1)} \right), \quad (3.9)$$

where we took NN interaction just as an example since the following discussion should be easily generalizable by the reader to further interactions. Thus, $\mathcal{H} = \sum_{m=0}^L \mathcal{H}_m$. Let us set $m = 1$ for a bit. The state resulting when \mathcal{H} acts on the momentum state 3.5, since $[\mathcal{H}, T] = 0$ is:

$$\mathcal{H}|\Psi(P)\rangle = \frac{1}{\sqrt{N_a}} \sum_{r=0}^{L-1} e^{-iPr} T^r \mathcal{H}|a\rangle = \frac{1}{\sqrt{N_a}} \sum_{m=0}^L \sum_{r=0}^{L-1} e^{-iPr} T^r \mathcal{H}_m|a\rangle, \quad (3.10)$$

and we need to operate with the Hamiltonian operators \mathcal{H}_m only on the representative state $|a\rangle$. For each operation, we get a different state, or, in the diagonal ($m = 0$) case, the same state. In either case we can write $\mathcal{H}_m|a\rangle = h_m(a)|b'_m\rangle$, where $h_m(a)$ is the matrix element coming from equations 3.8 and 3.9, and we do not, for simplicity of the notation, include any explicit indicator that $|b'_m\rangle$ also depends on $|a\rangle$. The prime in $|b'_m\rangle$ is there to indicate that this new state is not necessarily one of the reference states used to define the basis and, therefore, a momentum state should not be written directly based on it. If it is, instead, compatible with the momentum P , there should be a number l_m such that $|b_m\rangle = T^{l_m}|b'_m\rangle$ is fulfilled. Using this requirement, we can write

$$\mathcal{H}_m|a\rangle = h_m(a)T^{-l_m}|b_m\rangle, \quad l_m \in \{0, \dots, L-1\}, \quad (3.11)$$

where we have again simplified the notation by not making explicit the dependence of l_m on $|b_m\rangle$ (and thus on $|a\rangle$). We can now write equation 3.10 as

$$\mathcal{H}|\Psi(P)\rangle = \sum_{m=0}^L \frac{h_m(a)}{\sqrt{N_a}} \sum_{r=0}^{L-1} e^{-iPr} T^{r-l_m} |b_m\rangle, \quad (3.12)$$

which after shifting summation indices and taking into account the possible different normalization factors, we can extract the matrix elements of the Hamiltonian operators \mathcal{H}_m :

$$\langle \Psi(P) | \mathcal{H}_0 | \Psi(P) \rangle = \sum_{m=1}^L S_z^{(m)} S_z^{(m)}, \quad (3.13)$$

$$\langle b_m(P) | \mathcal{H}_{m>0} | \Psi(P) \rangle = e^{-iPl_m} \frac{1}{2} \sqrt{\frac{R_a}{R_{b_m}}}, \quad |b_m\rangle \propto T^{-l_m} \mathcal{H}_m |a\rangle, \quad (3.14)$$

where we have already substituted $h_m(a)$ for the specific Heisenberg model considered here. For a deeper discussion, consult [41].

This procedure is done by a program similar to the one used in section 3.1.1.1 but with several changes:

```

1   for i in (0, ..., length(basis)-1):
2       a = basis[i]
3       Ra = multiplicity(a)
4       state = binary(a, L)
5       for ii in (0, ..., L-1):
6           if state[ii] = state[ii+1]:
7               H[i, i] += 1/4
8           else:
9               H[i, i] -= 1/4
10              state' = flip(state, ii, ii+1)
11              b = representative(state')
12              Rb = multiplicity(state')
13              l = needed_to_reach(state', b)
14              j = index(b, basis)
15              if j >= 0:
16                  H[i, j] += 1/2 * sqrt(Ra/Rb) * exp(-iPl)

```

where we have already taken into account the matrix elements of equations 3.13 and 3.14. The program goes through the elements of the basis (of well-defined

momentum), generating a binary array `state` for each element via the function `binary` as before, and starts checking whether or not the bits `ii` and `ii+1` are equal. In the first case scenario, only the diagonal part $\propto S_z$ acts, while in the other both parts play their role. While the diagonal does not change the vector, the off-diagonal term $S_+S_- + \dots$ flips the bits, turning the bit `ii` into `ii+1` and viceversa generating thus a new binary array `state'` as previously in section 3.1.1.1. However, we now have to find the representative of the class in which this new state `state'` is (we may have jumped to another different class) as well as its properties. This is done via the functions `representative`, `multiplicity` and `needed_to_reach`, which compute, respectively, the representative `b` of the class in which the state `state'` is, its multiplicity `Rb` and how many times we need to use T to reach the representative `b` from `state'`. We then search in the basis via the function `index(b, basis)` that retrieves the position `j` of the representative `b` in the set `basis` unless it does not exist (it may not be allowed by the current chosen momentum, which would yield `j=-1`). This allows us to fill the entry `[i, j]` of the Hamiltonian in the case the `j` ≥ 0 . Note that in this example we only consider NN interaction as in the section 3.1.1.1. In order to go beyond, one would just have to add a new `for` loop that iterates over the values of the interactions (for instance, 1 and 2 for NN and NNN as in the J_2/J_1 models) modifying the contributions to the entries if anisotropies or different couplings were to be considered. Furthermore, as in the case of section 3.1.1.1, since our Hamiltonian matrix is in general hermitian (except when $P = 0$ or π , when it is real and symmetric) we could just store the elements above the diagonal, which will make faster the procedure. This is in fact what has been done in the actual code.

3.1.2 Additional symmetries

Apart from the symmetries already considered, there are a bunch more that, although have not been used in this work, are interesting to mention at least for the sake of completeness.

The first one is due to the commutation of the reflection R operator with any Hamiltonian made up of Heisenberg-like terms of the form of equation 2.4. This symmetry is the parity, defined by:

$$R|S_z^{(0)}, S_z^{(1)}, \dots, S_z^{(L-1)}\rangle = |S_z^{(L-1)}, \dots, S_z^{(1)}, S_z^{(0)}\rangle. \quad (3.15)$$

Its eigenstates $|\Psi(p)\rangle$ satisfy that, under the action of the translation operator T

on them we get: $R|\Psi(p)\rangle = p|\Psi(p)\rangle$, with $p = \pm 1$ since $R^2 = \mathbb{1}$. Note, however, that this symmetry can only be used in a sub-space of the full Hilbert space, since the commutation condition, namely $[R, \mathcal{H}] = 0$, is not always fulfilled. This leads to some subtleties, as the definition of the so-called *semi-momentum* states. The reader interested in it is encouraged to take a look at section 4.1.3 of [41]. Note also that in a system with open boundaries (not treated in this work) T is not well defined, while R -symmetry can still be exploited.

Another important symmetry coming from the fact that equation 2.4 is $SU(2)$ spin-rotationally invariant is the spin-rotation symmetry, which makes our Hamiltonian to commute with the quadratic spin operator $\vec{S} \cdot \vec{S}$ defined via

$$\vec{S} \cdot \vec{S} = \sum_{m=0}^{L-1} \vec{S}^{(m)} \cdot \vec{S}^{(m)}. \quad (3.16)$$

The action of this operator on its eigenstates is

$$\vec{S} \cdot \vec{S}|\Psi(S)\rangle = S(S+1)|\Psi(S)\rangle, \quad (3.17)$$

with S being the magnitude of the total spin of the many-body state. The fact that this operator can be cast in a Heisenberg-like form (meaning equal strength for interactions at all lengths) as follows

$$\vec{S} \cdot \vec{S} = \sum_{m=0}^{L-1} \sum_{n=0}^{L-1} \vec{S}^{(m)} \cdot \vec{S}^{(n)} = 2 \sum_{m < n} \vec{S}^{(m)} \cdot \vec{S}^{(n)} + \frac{3}{4}N, \quad (3.18)$$

makes the implementation of this symmetry a bit tricky and not as useful as one may imagine.

Finally, for the special (and most important since it is where the ground state lives) case null-magnetization sector (for even N), we can block-diagonalize using a discrete subset of all the possible rotations in spin-space: the spin-inversion symmetry, i.e. invariance with respect to flipping all the spins. This is defined formally by an operator Z such its action is

$$Z|S_z^{(0)}, S_z^{(1)}, \dots, S_z^{(L-1)}\rangle = |-S_z^{(0)}, -S_z^{(1)}, \dots, -S_z^{(L-1)}\rangle. \quad (3.19)$$

Similarly to the reflection operator, we again have $R^2 = \mathbb{1}$ and hence $z = \pm 1$. Although of easy implementation, it could not be added to the program due to lack of time and it will remain as a possible future extension to the work presented here in order to compute the ground state energy of higher size chains.

3.2 Diagonalization: Krylov space and the Lanczos procedure

Firstly, let us motivate the use of the Lanczos method using the words stated by Sandvik in [41]:

The number of operations needed to diagonalize an $M \times M$ matrix generally scales as M^3 , and the memory required for storage is $\approx M^2$ (even for a sparse matrix, as intermediate steps normally do not maintain sparsity).[...] Calculations aiming at just the ground state, and possible some number of excited states, can be carried out in other ways for larger systems, using, e.g. the Lanczos method.

Before entering into the rough explanation of the Lanczos method, we need to define the *Krylov space*. It is a sub-space of the full Hilbert space such that the low-lying eigenstates of a Hamiltonian \mathcal{H} are well approximated within it. It is constructed by acting Λ times with \mathcal{H} on an initial randomly-generated state $|\Psi\rangle$ in a M -dimensional Hilbert space. This procedure, if Λ is sufficiently large, will leave basically just the eigenstate with maximal eigenvalue E_{\max} , since in

$$\mathcal{H}^\Lambda |\Psi\rangle = \sum_{n=0}^{M-1} c_n E_n^\Lambda |\Psi_n\rangle = c_{\max} E_{\max}^\Lambda \left[|\Psi_{\max}\rangle + \sum_{n \neq \max} \frac{c_n}{c_{\max}} \left(\frac{E_n}{E_{\max}} \right)^\Lambda |\Psi_n\rangle \right], \quad (3.20)$$

only the term $\propto |\Psi_{\max}\rangle$ will survive provided that $c_{\max} \neq 0$, which is always feasible. If, as we want, we aim at the computation of the ground state $|\Psi_0\rangle$ we can just use $(\mathcal{H} - c\mathbb{1})^\Lambda$ (with $c > 0$ large enough to ensure the convergence to the desired state) or using \mathcal{H}^{-1} , since the maximum eigenvalue of a matrix is also the minimum of its inverse.

The Lanczos method's strength resides in the construction of an orthogonal basis, constructed by using linear combinations of the Krylov space states, such that the (symmetric) Hamiltonian written in this basis is tridiagonal (or, at least, it constructs a similar tridiagonal matrix to it). This makes the diagonalization procedure very fast and small-resource-demanding by, e.g. the Thomas algorithm.

In the computations done for this work, the author used an already built function called `eigsh`, developed for the `scipy.sparse.linalg` package in Python 3.0. This function is, as stated in its documentation¹ a wrapper to

¹ The documentation for the `scipy.sparse.linalg.eigsh` can be found in <https://docs.scipy.org/doc/scipy-0.14.0/reference/generated/scipy.sparse.linalg.eigsh.html> (consulted on 19/08/2017).

the ARPACK² SSEUPD and DSEUPD functions which use the Implicitly Restarted Lanczos Method to find the eigenvalues and eigenvectors [42]. Previous work specifically designed for spin chains in Fortran77 as *TITPACK* can be found at [24].

3.3 Density matrices and tracing over subspaces

After using the Lanczos method implemented by the built-in function `eigsh` in Python's package `scipy`, we get the expression of the ground state $|\Psi_0\rangle$ in terms of the well-defined momentum basis $\{|\Psi(P)\rangle\}$, so the first step is to convert it back to the computational 2^L -dimensional basis using the function `to_spinbasis` which is defined as follows:

```

1  to_spinbasis(state,P,L,S,R):
2      for i in (0,...,length(S)-1):
3          for ii in (0,...,L-1):
4              state'[T^ii(S[i])] += ...
5                  state[i] * sqrt(R[i]/L^2) * exp(-I P))
6  return state'
```

We pass to the function a vector S containing the representatives of the different classes and a vector R with their respective multiplicities. They both will be used to convert the initial ground state in the momentum basis `state` to the computational 2^L -dimensional basis `state'` iterating over the elements of the basis and using the translation operator T `ii` times. Once we have the array `state'` containing the ground state $|\Psi_0\rangle$ as we want, we form the whole density matrix ρ just using its general definition for an arbitrary state $|\psi\rangle$:

$$\rho = |\psi\rangle \otimes \langle\psi|. \quad (3.21)$$

From this monstrous matrix describing the whole system \mathcal{S} , we define the reduced density matrix ρ_A over the subspace A by tracing over its complementary subspace B , that is $A \cup B \equiv \mathcal{S}$, as

$$\rho_A = \text{Tr}_B \rho. \quad (3.22)$$

Although formally perfect, this amounts to say that we write the components

² Consult the ARPACK page: <http://www.caam.rice.edu/software/ARPACK/> (retrieved on 19/08/2017).

of the state $|\psi\rangle$ as tensor products made up by states of the subspace A with states of the subspace B and only keep the components that, after performing the Kronecker product of equation 3.21, are diagonal. This procedure, although easy to work out by hand and pencil, is not as simple for a computer. The function that computes a reduced density matrix `rhof` for a subchain of length `l` given a whole density matrix `rho` of a chain of length `L` is the following:

```

1  rho_red(rho, L, l):
2      position = (0,0)
3      for i in (0, ..., 2^L-1):
4          for j in (0, ..., 2^L-1):
5              n = i*2^L + j
6              condition = extract_pos(n, l, L, position)
7              if condition:
8                  rhof[position[0], position[1]] += rho[i, j]
9              position = (0,0)
10     return rhof

```

This function iterates over all the entries of the whole matrix `rho` and decides whether or not each entry must be added (and where to do so) to the final reduced density matrix `rhof`. This process is done via the sub-process `extract_pos` that returns a boolean variable `condition` for the decision-making process and changes the value of the pair `position` to know which entry of `rhof` must be modified. The sub-process `extract_pos` is described by:

```

1  extract_pos(n, l, L, position):
2      V = to_bin(n, 2L)
3      v = zeros(2l)
4      a = zeros(L-1)
5      b = zeros(L-1)
6      for i in (0, ..., L-1-1):
7          a[i] = V[2L-1-1-i]
8          b[i] = V[L-1-1-i]
9      condition = 0
10     if(want_it(a, b)):
11         condition = 1
12         for j in (0, ..., l-1):
13             v[j] = V[2L-1-j]
14             v[j+1] = V[L-1-j]

```

```

15     position[0] = floor(to_dec(v) / (2^l))
16     position[1] = mod(to_dec(v), 2^l)
17     return condition

```

This function starts by creating some null arrays of different lengths and creating a binary array with $2L$ entries with its bits describing the number n in a binary basis using a simple `to_bin` function (which is included in most of the programming languages and will not be described here). This number n computed previously in the function `rho_red` is precisely the one that once is translated into the spin basis yields the chain of bits formed by the product of equation 3.21. Let us see this with an example. Take $L = 3$ such that ρ is a 8×8 square matrix and chose, e.g. the entry at row 0 and column 5 (we are using here the convention followed by most of the programming languages), yielding $n = 0 \times 2^3 + 5 = 5$. Converting it into a binary basis using a chain of $2L = 6$ bits gives (000101), which is exactly the origin of this entry when looking at the definition of the ρ matrix in equation 3.21, i.e. $|000\rangle_b \otimes \langle 101|_b$. Now, it takes the first $L-1$ bits of each set of L (with l being the length of the subchain for which we want to compute ρ_{red}) and stores them into the two arrays `a` and `b`. Once both arrays are filled properly, we decide whether this entry must be consider when doing the trace over the subspace, which is decided by the sub-process `want_it` that simply checks whether the arrays `a` and `b` are exactly equal or different, which will lead to keep it or not respectively, returning the value 1 or 0 for each case respectively. If `a=b`, the function sets the boolean variable `condition` to 1, which will be used in the main process `rho_red`, and computes the position of the entry of the reduced density matrix ρ_{red} to which the considered entry of the full density matrix ρ will be added, using for this computation the remaining bits extracted from `v` and neither stored in `a` nor in `b` previously. For this final part, the function uses the well-known commonly built-in functions in most programming languages `mod` and `floor` that compute the modulus and the integer part of a division respectively. It also uses a simple function `to_dec` with which the binary chain `v` is transformed into a decimal number.

4

Theoretical predictions and formulae

4.1 Finite size scaling

In the rather important paper by Affleck *et al.* [17], whose ideas were introduced and briefly reviewed in section 2.2.4, it is stated that a spin-1/2 Heisenberg anti-ferromagnetic chain described by a typical $J_2/J_1 \approx 0.25$ model of equation 2.2 (in comparison to XXX Hamiltonian of equation 2.1 with $\Delta = 1$) is well described by a CFT with central charge $c = 1$ that can be identified with a $SU(2)_{k=1}$ WZW non-linear σ -model. This confers a characteristic nature to the energies of the ground and excited states.

It can be proved that, even though the ground state energy is not universal, their corrections are, and the scaling of the energy of any state in a chain of length L with Fermi velocity v and described by a CFT with central charge c and primary fields with conformal weights h and \bar{h} is given by:

$$E(L) = e_0 L - c \frac{\pi v}{6L} + \frac{2\pi v}{L} (h + \bar{h}), \quad (4.1)$$

where e_0 is just a constant. In our case, as explained in [17] and summarized in section 2.2.4, the primary fields are given in terms of the left and right spin Casimirs: $h = S_L^2$ and $\bar{h} = S_R^2$.

Following from here, it can be shown that the ground state energy $E_0(L)$ of a

chain of L spins described by these theories is given by

$$E_0(L) = e_0 L - c \frac{\pi v}{6L} + \dots, \quad (4.2)$$

with the \dots meaning higher-order corrections and the constant e_0 expected to be fitted numerically and agreed with the Bethe Ansatz prediction for the XXX model ($J_2/J_1 = 0$): $e_0 \approx \ln 2 - 1/4 \approx 0.44315$. Affleck *et al.* also give a complete formula for $E_0(L)$ in [17] that takes into account the higher-order terms, namely:

$$E_0(L) \approx e_0 L - \left(\frac{\pi}{6L} \right) \left[\frac{3k}{2+k} + \frac{3k^2}{8(\ln L)^3} \right]. \quad (4.3)$$

Note how the central charge c appears via equation 2.22 inside the bracket. Substituting $k = 1$ into equation 4.3 and dividing by the length L :

$$\frac{E_0(L)}{L} \approx e_0 - \left(\frac{\pi v}{6L^2} \right) \left[1 + \frac{3}{8(\ln L)^3} \right], \quad (4.4)$$

which will be the equation that will be verified numerically, whose results appear in section 5.1. The corrections $\sim 1/(L(\ln L)^3)$ to the energy are due to the perturbations originated by a *marginally irrelevant* operator¹, which induces a flow away from the universality class of the CFT corresponding to the WZW $SU(2)_{k=1}$ model, which is the continuum limit of the XXX Heisenberg model as it has been discussed previously in this work. We will see this flow away from the universality class by obtaining the energy of the ground state $E_0(L)$ for various lengths L and values of J_2/J_1 in the range $[0, 0.25]$, given that both points are well described by the continuum limit CFT.

4.2 Spectrum and Conformal towers

Going back now to equation 2.18, in which the Hamiltonian is written in terms of the chiral components of the energy-momentum tensor, and taking into account the expression 4.1 of the previous section for the energy of excited states in a spin chain of length L , it can be argued that the scaled-differences in energy of the first excitations with respect to the ground state energy $E_0(L)$ are distributed along spin multiplets with different degeneracies. This, following the discussion of [17], introduced in 2.2.4, can be seen in tables 4.1 and 4.2.

¹Consult section A.1 to find the definition of this type of operators in the context of renormalization.

$\Delta E(L/(2\pi v))$	$s = 0$	$s = 1$	$s = 2$
4	2	3	1
2	1	1	1
0	1		

Table 4.1: Degeneracies of total spin multiplets for $k = 1$ and $P = 0$.

$\Delta E(L/(2\pi v))$	$s = 0$	$s = 1$	$s = 2$	$s = 3$
9/2	2	4	3	1
5/2	1	1		
1/2	1	1		

Table 4.2: Degeneracies of total spin multiplets for $k = 1$ and $P = \pi$.

As it is said in 2.2.4 related to the discussion of equation 2.16 for the scaling dimension x of the primary fields, the case $P = 0$ ($P = \pi$), of table 4.1 (4.2), corresponds to conformal towers formed by applying lowering operators to the highest-weights states with spins $s_{L_0} = s_{R_0} = 0$ ($s_{L_0} = s_{R_0} = 1/2$).

Note that in both cases the Fermi velocity v appears. Although in the XXX model (solvable by the Bethe Ansatz [3]) has a value of $\pi/2$ in the limit $L \rightarrow \infty$, in our case has to be numerically fitted to obtain the values of the table (as explained in section 5.2), something which is not normally mentioned in the literature, as in [17]. The variation of this velocity v will be studied in the results related to the scaling of the energies, of section 5.1. The numerical results that confirm completely the structure of the conformal towers can be seen in section 5.2.

4.3 Correlators and exchange-size dependence

The first logarithmic corrections to the scaling of the energies and to the correlation functions, being the latter what concerns us in this section, were obtained by Affleck *et al.* in 1989 [17] applying CFT to WZW non-linear σ -models as explained in sections 2.2.3 and 2.2.4. As it is said in [43], although this theoretical development soon motivated numerical analysis, they were inconsistent between the different results.

Some notorious ones, carried by Kaplan and co-workers [44] or Lin and Campbell [45] among others, obtained the following formula:

$$\langle S_i^{(0)} S_i^{(r)} \rangle \approx \frac{(-1)^r \ln^\sigma(r)}{r}, \quad (4.5)$$

with $i = \{x, y, z\}$, and r being the exchange interaction distance. Here, σ was

found to be in the interval $0.2 < \sigma < 0.3$. However, better numerical results obtained by the DMRG procedure developed by White [26], allowing higher sizes of the chains non-reachable previously by Lanczos methods, confirmed finally the formula predicted by Affleck *et al.* in his 1989's paper [11], whose version was improved afterwards and written as [29]:

$$\langle S_z^{(0)} S_z^{(r)} \rangle = \mathcal{C} (-1)^r \frac{\sqrt{\ln r}}{r} - \frac{1}{4\pi^2} \frac{1}{r^2} + \dots, \quad (4.6)$$

with the expectation value (the correlator) computed at the ground state $|\Psi_0\rangle$ and \mathcal{C} being just a constant to be determined numerically. Note that due to rotational invariance, $\langle \vec{S}^{(0)} \vec{S}^{(r)} \rangle = 3 \langle S_z^{(0)} S_z^{(r)} \rangle$.

Equation 4.6 corresponds to the limit $L \rightarrow \infty$. If one instead wants, as it is our case, a finite-size PBC formula, one must do the substitution

$$r \rightarrow \frac{L}{\pi} \sin \frac{r\pi}{L}, \quad (4.7)$$

valid for $r \ll 1$. With this substitution, equation 4.6 converts into

$$\langle S_z^{(0)} S_z^{(r)} \rangle = \mathcal{C} (-1)^r \frac{\sqrt{\ln \left(\frac{L}{\pi} \sin \frac{r\pi}{L} \right)}}{\left| \frac{L}{\pi} \sin \frac{r\pi}{L} \right|} - \frac{1}{4\pi^2} \frac{1}{\left(\frac{L}{\pi} \sin \frac{r\pi}{L} \right)^2} + \dots, \quad (4.8)$$

which will be the equation that will be verified numerically in section 5.3, by exact diagonalization results. This will allow us to see how the correlators vary when we move away from the critical CFT $c = 1$ point, i.e. $J_2/J_1 \approx 0.25$ in J_2/J_1 model of equation 2.2, and determine the importance of the corrections. These variations of the correlators are due to the fact that at the XXX model or isotropic point $\Delta = 1$ for the XXZ model, irrelevant operators become marginal, yielding logarithmic corrections [34].

4.4 Entanglement entropies and Quantum Information

The α -Rényi entropies $S_R^{(\alpha)}$ of a system described by a density matrix ρ can be used as a measure of the degree of entanglement present in a system. They are defined as:

$$S_R^{(\alpha)} \equiv \frac{1}{1-\alpha} \ln \text{Tr} \rho^\alpha = \frac{1}{1-\alpha} \ln \left(\sum_i \lambda_i^\alpha \right), \quad (4.9)$$

with λ_i being the eigenvalues of ρ . This is somehow a general extension of the well-known Von Neumann entropy defined by

$$S_{VN} = -\text{Tr}(\rho \ln \rho), \quad (4.10)$$

since for $\alpha \rightarrow 1$ in equation 4.9, we recover the Von Neumann entropy S_{VN} .

As mentioned in the introduction, in 1994, Holzhey, Larsen, and Wilczek [18], who were interested in the study of black holes, derived the first formula for entropies of a system of finite size l described by a CFT with central charge c :

$$S(l) \simeq \frac{c}{3} \ln l \quad (4.11)$$

However, Vidal *et al.* soon realized those equations could be applied to low-dimensional Physics, more concretely to spin chains [19]. They used the substitution previously mentioned in equation 4.7 to obtain instead:

$$S(l) \simeq \frac{c}{3} \ln \left[\frac{L}{\pi} \sin \left(\frac{\pi l}{L} \right) \right]. \quad (4.12)$$

Some years later, this formula was generalized by Calabrese *et al.* [22] for the α -Rényi entropies $S^{(\alpha)}(l)$ of the subchain with integer length l to incorporate parity effects, obtaining:

$$S^{(\alpha)}(l) = S_{CFT}^{(\alpha)}(l) + \text{corrections}, \quad (4.13)$$

$$S_{CFT}^{(\alpha)}(l) = \frac{c}{6} \left(1 + \frac{1}{\alpha} \right) \ln \left[\frac{L}{\pi} \sin \left(\frac{\pi l}{L} \right) \right], \quad (4.14)$$

$$\text{corrections} = c'_\alpha + f_\alpha \cos(2k_F l) \left| 2 \frac{L}{\pi} \sin \left(\frac{\pi l}{L} \right) \sin(k_F) \right|^{-p_\alpha}, \quad (4.15)$$

with c being the central charge of the CFT in the critical point (given in our case by 2.22) and c'_α and f_α being two parameters to be determined by numerical fitting of the points. In our case, as explained in the reference [22], they are given by

$$k_F = \pi/2, \quad (4.16)$$

$$K = 1/2, \quad (4.17)$$

$$p_\alpha = 2K/\alpha. \quad (4.18)$$

The parameters K and k_F are the *Luttinger liquid parameter* and the *Fermi momentum* respectively [22], and p_α is a universal critical exponent of the theory.

Substituting these results into equations 4.14 and 4.15 and fixing $c = 1$ one

obtains for $\alpha = 2$, which is the simplest case one can study, the formula:

$$S^{(2)}(l) = \frac{1}{4} \ln \left[\frac{L}{\pi} \sin \left(\frac{\pi l}{L} \right) \right] + c'_2 + f_2 \frac{(-1)^l}{\sqrt{\left| 2 \frac{L}{\pi} \sin \left(\frac{\pi l}{L} \right) \right|}}, \quad (4.19)$$

which will be verified numerically in section 5.4 and used to obtain the different fitting parameters c'_2 and f_2 and their variations in the range $J_2/J_1 \in [0, 0.25]$, whose extrema are well described by a CFT with $c = 1$.

4.5 Haldane-Shastry model and its relation to J_2/J_1 model

The Haldane-Shastry model is an interesting case of study by itself, since it is one of the cases in which one can find an analytical solution for a many-body problem in Quantum Mechanics [46]. It is described by the following Hamiltonian [27, 28]:

$$\mathcal{H}_{HS} = J \sum_{i < j} \left(\frac{\pi}{L} \right)^2 \frac{\vec{S}^{(i)} \cdot \vec{S}^{(j)}}{\sin^2 \left(\frac{\pi(i-j)}{L} \right)}. \quad (4.20)$$

The term $i - j$ inside the argument of the sine appearing in the denominator of each individual term plays the role of a distance, that weights proportionally the interactions to simulate a more realistic case in which the further two spins are from one another, the weaker their interaction is.

The analytical solution for the ground state of this Hamiltonian can be obtained [46]. If a generic state of a spin-1/2 chain with L particles has the form

$$|\Psi\rangle = \sum_{s_0, \dots, s_{L-1}} \Psi(s_0, \dots, s_{L-1}) |s_0, \dots, s_{L-1}\rangle \quad (4.21)$$

when expressed in a local spin basis $\{|s_m\rangle\}$, where $s_m = \pm 1/2$ and $m \in [0, L - 1]$, the coefficients that yield the ground state wavefunction $|\Psi_0^{(HS)}\rangle$ of the Haldane-Shastry Hamiltonian \mathcal{H}_{HS} of equation 4.20 can be shown to be:

$$\Psi_0^{(HS)}(s_0, \dots, s_{L-1}) \propto \exp \left[i\pi \sum_{\text{odd } i} (s_i - 1/2) \right] \prod_{n < m}^{L-1} \left[\sin \left(\frac{\pi(n-m)}{L} \right) \right]^{2s_n s_m}, \quad (4.22)$$

where we assumed that the ground state lives in the Hilbert subspace of null magnetization, i.e. $\sum_{m=0}^{L-1} s_m = 0$.

A schematic view of how the terms are included in the sum of equation 4.20

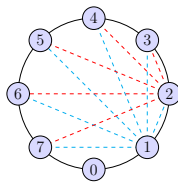


Figure 4.1: Schematic showing how the interaction goes in the Haldane-Shastry model defined in equation 4.20 for a spin chain of length $L = 8$. Spins appear numbered by their index i in the sum, and terms for $i = 1$ (2) appear denoted as dashed coloured blue (red) lines connecting the interacting spins.

appears in figure 4.1, in which the terms for $i = 1$ and $i = 2$ appear denoted by dashed lines of blue and red colours respectively. Note that in the $i = 2$ case, no red line appears for the $1 - 2$ interaction, since it was already taken into account.

One very interesting property of the Hamiltonian \mathcal{H}_{HS} , using definition 4.20, is that when the distance is very small (naturally speaking of a very large ring), namely, $\frac{\pi}{L}(i - j) \approx 0$, one can take $\sin(x) \approx x$ for $x \approx 0$, which allows us to write equation 4.20 as

$$\mathcal{H}_{HS} \approx J \sum_{i < j} \frac{\vec{S}^{(i)} \cdot \vec{S}^{(j)}}{(i - j)^2} = J \sum_{i=0}^{L-1} \left(\vec{S}^{(i)} \cdot \vec{S}^{(i+1)} + \frac{1}{4} \vec{S}^{(i)} \cdot \vec{S}^{(i+2)} + \dots \right), \quad (4.23)$$

which resembles us a lot to the Hamiltonian \mathcal{H}_{J_2/J_1} of the J_2/J_1 model (equation 2.2) with the very particular value $J_2/J_1 = 0.25$, which is approximately equal to the critical point where this model is described by a CFT with central charge $c = 1$. This leads us to think that we should see some kind of logarithmic scaling behaviour [46] of the overlap between the ground states of the Heisenberg XXX model and the Haldane-Shastry model while the overlap between the latter and the ground state of the $J_2/J_1 = 0.25$ model should be close to unity, namely:

$$|\langle \Psi_0^{(XXX)} | \Psi_0^{(HS)} \rangle| \longrightarrow 0, \quad (4.24)$$

$$|\langle \Psi_0^{(J_2/J_1=0.25)} | \Psi_0^{(HS)} \rangle| \longrightarrow 1. \quad (4.25)$$

The tendency of the first equation could be $\sim 1/L^x$ with x a critical exponent, or even slower: $\sim 1/(\ln L)^x$. These overlaps will be studied numerically in section 5.5 for a range of values of J_2/J_1 . Note that the tendencies discussed here would only apply for a limited value of lengths, given that in the thermodynamic limit, overlaps from many-body wavefunctions as the ones used here, always go to 0, so in principle, we may not find the tendency of equation 4.25.



Results and discussion

In this section, the numerical results obtained in order to verify the different equations and predictions appearing all throughout this work are presented and discussed. It will be found that, indeed, the description of XXX spin chains and $J_2/J_1 = 0.25$ models are correctly represented by the corresponding field theory in the continuum limit, i.e. the $SU(2)_{k=1}$ WZW model.

5.1 Finite size scaling

In order to prove that the identification of the critical theory as well as the general principles of conformal field theory, one of the most accessible things one can do is to see whether the prediction for the ground state energy from the theory match those of real computations. To do so, we generate the Hamiltonian \mathcal{H}_{J_2/J_1} for different values of the ratio J_2/J_1 and for different total lengths L of the chains, using the methods described in section 3. Once it is done, we find their minimum eigenvalue via the Lanczos method, and hence the different ground state energies per site $E_0(L)/L$ can be computed.

The results appear in figure 5.1, where two curves from the prediction of equation 4.4 have been plotted to show how good the agreement with the theory is. The purple solid curve has as its parameters e_0 , k and v the predictions from the Bethe Ansatz, i.e. $e_0 \approx 1/4 - \ln 2 \approx -0.443$, $k = 1$ and $v = \pi/2 \approx 1.57$, and match perfectly the points of the XXX model ($J_2/J_1 = 0$). The red dashed curve

tries to fit (not almost perfectly as it can be seen due to the point of smallest L) the data points for the $J_2/J_1 = 0.25$ case, which is also another critical point. The values obtained in this case for (e_0, k, v) were $(-0.4007, 1, 1.08)$, as appears (together with all the remaining cases) in table 5.1. As it is understandable, the term proportional to k^2 in equation 4.4, which yields the $1/(\ln L)^3$ correction, played a minor role due to the small sizes reached in this work, and hence no appreciable differences were seen in the curves and fits varying the value of k , so it remained $k = 1$ in all the cases.

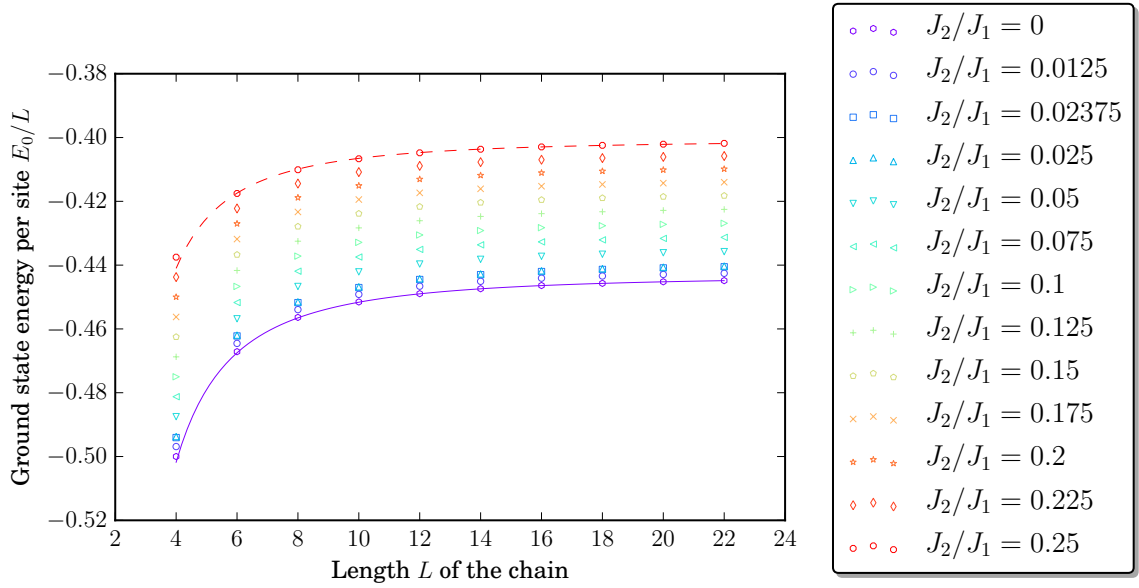


Figure 5.1: Ground State energy scaling with the length of the ring for different J_2/J_1 models. The purple solid curve is computed using the values obtained from the Bethe Ansatz as discussed in [17], i.e. $e_0 = 1/4 - \ln 2 \approx -0.44315$, $k = 1$, and $v = \pi/2$, while the red dashed one has numerically-fitted parameters, as appearing in table 5.1

5.2 Spectrum and Conformal towers

The results presented here in figure 5.2 are completely consistent with the results obtained by Affleck *et al.* in [17], showing in a more detailed manner the distinct spin-multiplets and the conformal structure of the low-excitations of a Heisenberg ring of spin-1/2 particles whose interaction is governed by two different Hamiltonians, the so-called XXX model (equation 2.1 with the anisotropy coefficient $\Delta = 1$) and the J_2/J_1 model (2.2) with a particular value for the ratio of the two couplings.

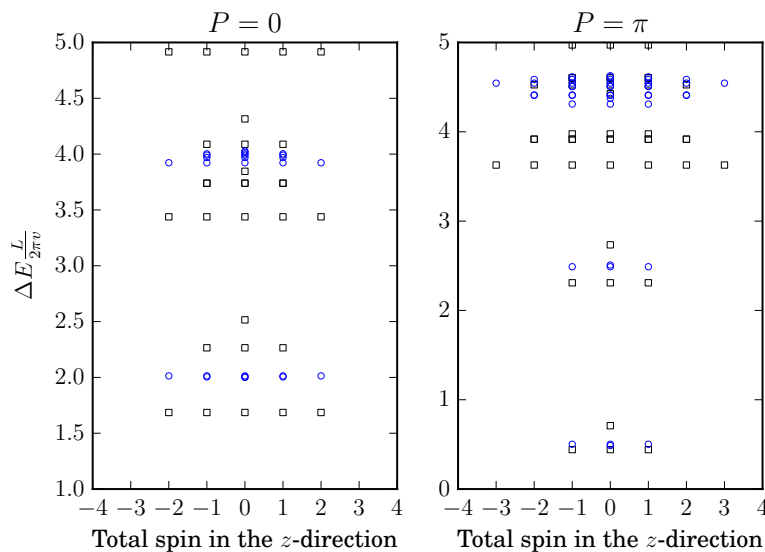


Figure 5.2: Spectrum showing the Conformal Towers of a 20 spin ring governed by a Hamiltonian of the form of equation 2.2. The left (right) panel shows the difference in energy with respect to the ground state energy for states with momentum $P = 0$ ($P = \pi$), scaled by a coefficient $\frac{L}{2\pi v}$, where L is the length of the chain (i.e., 20) and v being the *Fermi* velocity, fitted numerically. The hollow blue spheres (black squares) are the values obtained for the $J_2/J_1 = 0.25$ ($J_2/J_1=0$) case. The values of v that are used appear in table 5.1.

To obtain the data, we generated momentum-fixed-Hamiltonians for the cited models in all the possible magnetization sectors, and obtained their minimum eigenvalue. Due to the almost perfect degeneracy of some multiplets, it is difficult to see the different states. For instance, the predictions of the CFT with $c = 1$ of table 4.1, which says that we should have three states of spins 0,1, and 2, with $\Delta E \frac{L}{2\pi v} = 2$, agree with our results, since $1+3+5=9$ states appear in the left plot.

In order to fit the data to the corresponding CFT predictions in the J_2/J_1 case, remember that for the XXX case $v = \pi/2$, the coefficient v was fixed. However, the fitting required in the previous section to study the scaling of the ground state energy per site $E_0(L)/L$ was seen to agree with the value obtained independently for the conformal towers.

As it is discussed in [17], the large degeneracy of states at higher energies is due to the $SU(2) \times SU(2)$ symmetry of the critical theory. The small splittings of the supermultiplets are not determined by marginal operators but by marginally irrelevant ones, that induces a flow away from the critical point.

5.3 Correlators and exchange-size dependence

One of the most important results of a CFT is how easily correlators of physical operators can be computed. In particular, in our case, given that the operators $S_z^{(r)}$ have a quick-to-compute action on a given state, it is easy to simulate it numerically once one has the corresponding state over which one wants to act. The correlators are computed using the ground state wavefunction, which is obtained as the eigenvector with lowest eigenstate of the Hamiltonian matrix generated. We obtained results for a range of total lengths L varying between 4 and 22, begin the latter the case presented in this section in figure 5.3.

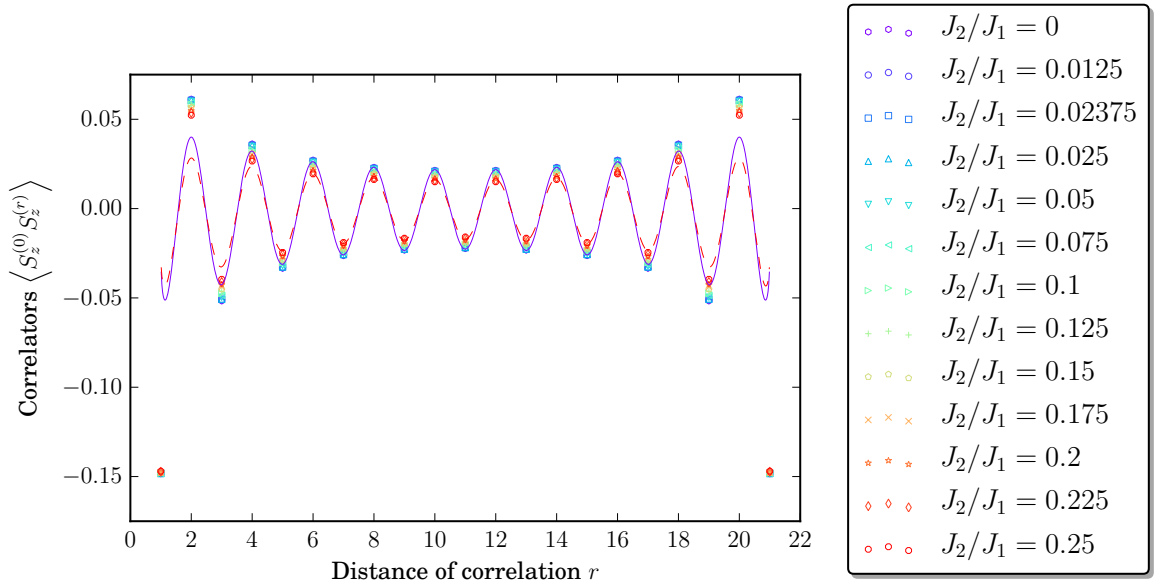


Figure 5.3: Variation of the correlators $\langle \Psi_0 | \vec{S}^{(m)} \cdot \vec{S}^{(m+r)} | \Psi_0 \rangle$ with respect to the distance of correlation r for a chain of length $L = 22$ in different J_2/J_1 models. The values were computed using the Lanczos-method-computed ground state $|\Psi_0\rangle$ from the Hamiltonian for the reduced Hilbert space of fixed magnetization and momentum. Purple solid (red dashed) curve is a numerical fitting to equation 4.8 for $J_2/J_1 = 0$ (0.25).

The purple solid (red dashed) curve is the numerical fit to equation 4.8 of the data points for different values of the ratio J_2/J_1 obtaining hence the constant parameter \mathcal{C} , whose values appear in table 5.1. It is interesting to note that the points do not seem to diverge a lot from different values of the ratio J_2/J_1 , and that the fits match better the oscillations the higher the distance of correlation r is. Once again, as in the previous sections, the predictions of the theory seem to agree very well with the numerical results, showing an almost linear behaviour for the parameter \mathcal{C} as a function of the ratio: $\mathcal{C}(J_2/J_1) \approx 0.1114 - 0.1122 (J_2/J_1)$.

5.4 Entanglement entropies and Quantum Information

Following a procedure similar to the one described in the previous section, we obtained the eigenfunction corresponding to the minimum eigenvalue of the generated Hamiltonian matrices for different lengths L and ratios J_2/J_1 . However, only the results of the maximum allowable size, $L = 12$, will be presented, since the agreement with the predictions of the theory are better the higher L is. Note that although in the previous case the maximum allowable size was $L = 22$, now L is smaller. This is due to the fact that in order to compute the entropies, once the eigenfunction is obtained in the basis of fixed magnetization and momentum, we must construct the density matrix ρ . This density matrix is built in the spin basis of size 2^L , and memory requirements soon start to be too demanding on the resources available for this work. Thus, although higher total L sizes were reachable, it was not possible to construct the corresponding ρ matrix.

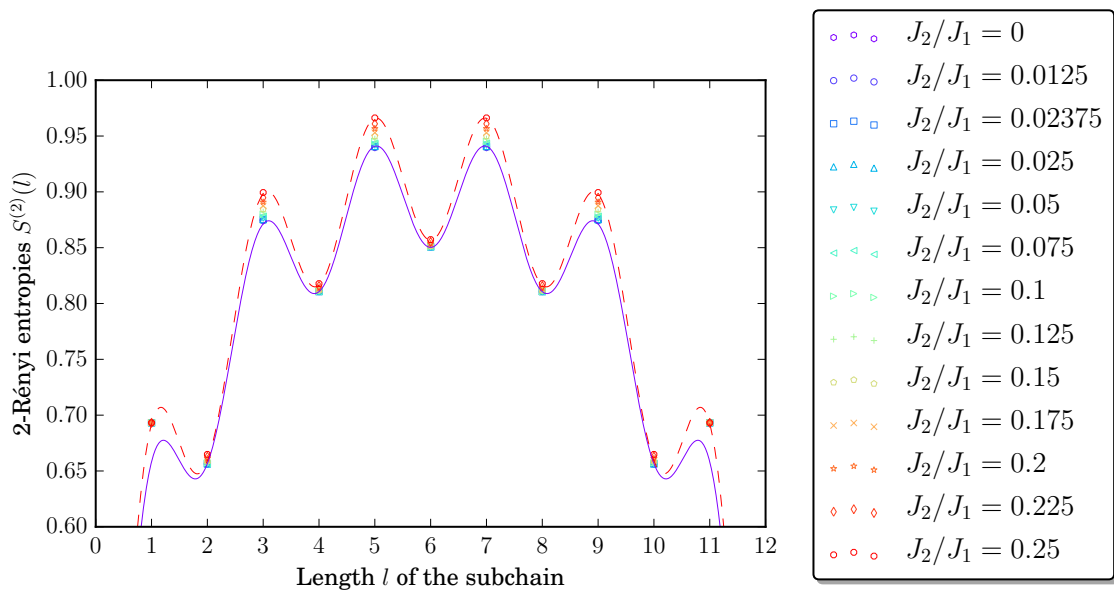


Figure 5.4: Entropy of entanglement between different length subchains of a ring of length $L = 12$ in different J_2/J_1 models. The panel shows the 2-Rényi entropies obtained by exact diagonalization of the density matrix for the ground state. Purple solid (red dashed) curve is a numerical fitting to equation 4.19 for $J_2/J_1 = 0$ (0.25). Note the oscillations and how well they fit to the theoretical curve proposed in [22], i.e. equation 4.19.

In the case presented here, i.e. $L = 12$, completely diagonalizing the density matrix ρ associated to the ground state allows us to compute its eigenvalues,

with which the different Rényi and Von Neumann entropies of equations 4.9 and 4.10, respectively, can be calculated. The results are presented in figures 5.4 and 5.5 respectively for a variety of J_2/J_1 ratios, containing both the limiting cases $J_2/J_1 = 0$ (the XXX model) and $J_2/J_1 = 0.25$ that admit a description by a CFT with $c = 1$.

While in the former case the oscillations due to parity effects [22] are perfectly seen, they do not exist in the Von Neumann case. In both cases, the purple solid (red dashed) curves stand for the fit to equation 4.19 (4.12), obtaining values for the parameters c_2 and f_2 (c and *shift*). The parameter *shift* is just a constant that is being added to equation 4.12 in order to fit the points. It is interesting to note that in the Rényi entropies case, we kept fixed $c = 1$ and obtained the other parameters since the action of c was very subtle, while in the Von Neumann case we use c as a parameter. As one can see by rapid inspection of the values of c in table 5.1, we could in principle take instead $c = 1$ for the Von Neumann case, and argue that the difference could be due to marginal operators appearing when moving out of the critical theory.

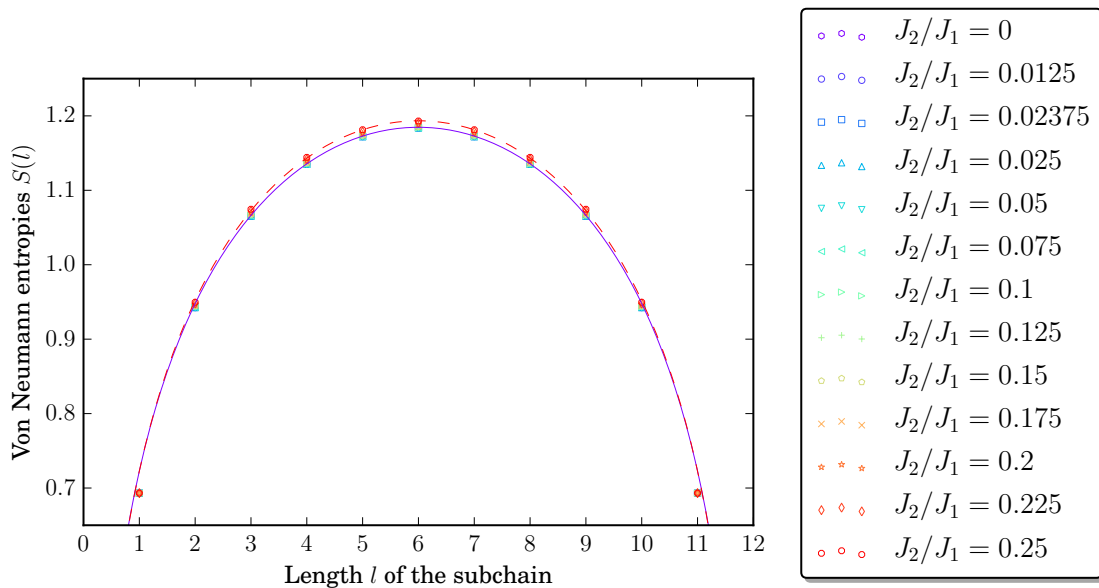


Figure 5.5: Entropy of entanglement between different length subchains of a ring of length $L = 12$ in different J_2/J_1 models. The panel shows the Von Neumann entropies obtained by exact diagonalization of the density matrix obtained from the ground state. Purple solid (red dashed) curve is a numerical fitting to equation 4.12 for $J_2/J_1 = 0$ (0.25). Note that in this case, compared to that one of figure 5.4, no oscillations are present. However, we still find an acceptable fit by the finite version of the first equation proposed by Holzhey *et al.*, i.e. equation 4.12 by Vidal *et al.*

Concerning the results for the fits in both cases (and all the numbers appearing in table 5.1), we can say that the predictions of the theory agree with the results. However, it is in both cases that when considering the smallest possible subchain, i.e. of length $l = 1$, the data points are harder to adjust, and one must pay more attention to the oscillations in the central area than to the external ones.

5.5 Haldane-Shastry model and its relation to J_2/J_1 model

The discussion that led to equation 4.23 in section 4.5 induced us to think that the overlap between the ground state wavefunction of the Haldane-Shastry Hamiltonian with that one of the J_2/J_1 model should be close to 1 for $J_2/J_1 = 0.25$ and much smaller for the XXX case.

In this work, we followed two distinct paths: generating the Haldane-Shastry Hamiltonian matrix and use the Lanczos method to obtain its ground state, or generating the ground state via the analytical solution of equation 4.22. The results are presented in figure 5.6 for the first case, while in figure 5.7 for the second one. Note that the maximum size reached following the first approach is only 12 due to similar reasons discussed when speaking about the results of entanglement entropies and the generation of the density matrix. Besides, notice that the agreement between the two approaches is excellent, what allows us to convince ourselves that the analytical solution holds.

Using the results from the overlap with the numerical generation of the analytical solution, we could analyse whether or not the behaviour predicted in equations 4.24 and 4.25 for the respective overlaps appears. Although it is easy to see that there is indeed a decay law, it does not have any of the forms already mentioned, namely $\sim 1/L^x$ or $\sim 1/(\ln L)^x$. We can instead, fitting the data for the two extremal points $J_2/J_1 = 0$ (corresponding to the XXX model) and $J_2/J_1 = 0.25$ to a polynomial ansatz of the form:

$$|\langle \Psi_0^{(J_2/J_1)} | \Psi_0^{HS} \rangle| = \sum_{i \in \mathbb{Z}} a_i L^i. \quad (5.1)$$

Doing so, we obtain the parameters $\{a, b, c, d\}$ that appear in table 5.1 for a whole range of values of J_2/J_1 , which are used in the extremal cases mentioned above to plot the purple solid and red dashed curves. It is notorious that they cross each other at $L = 14$, which was not expected. Note also that no terms with $i > 3$ in the sum 5.1 were required.

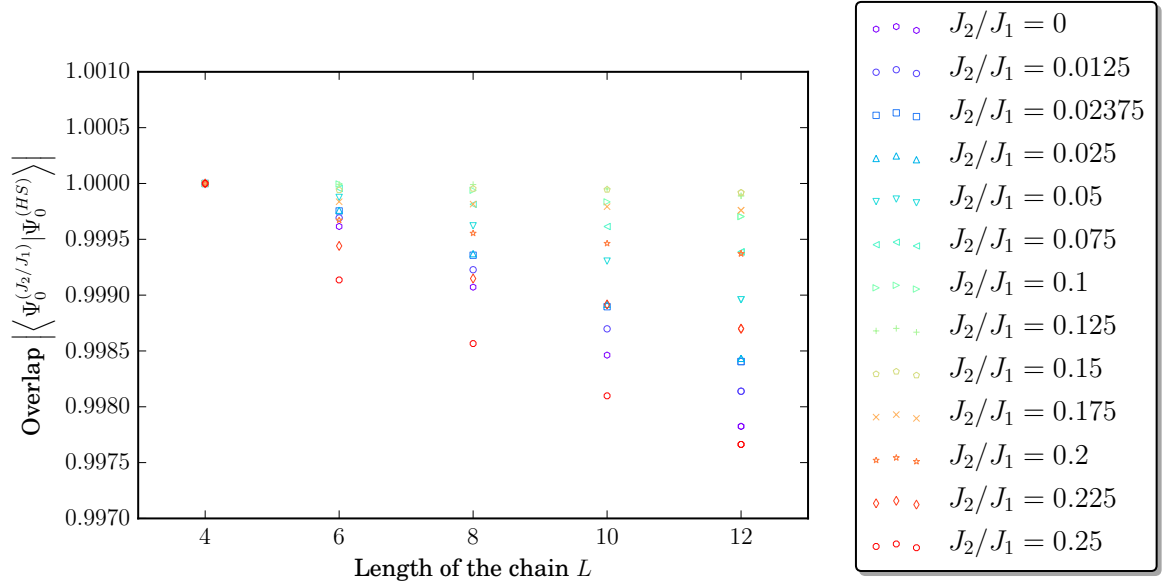


Figure 5.6: Variation with respect to the value of J_2/J_1 for the overlap between ground states of the Haldane-Shastry Hamiltonian \mathcal{H}_{HS} defined in equation 4.20 and the J_2/J_1 Hamiltonian computed via the formula $|\langle \Psi_0^{(J_2/J_1)} | \Psi_0^{HS} \rangle|$ for different J_2/J_1 models. These results were obtained using a numerical diagonalization for the computer-generated Hamiltonian \mathcal{H}_{HS} .

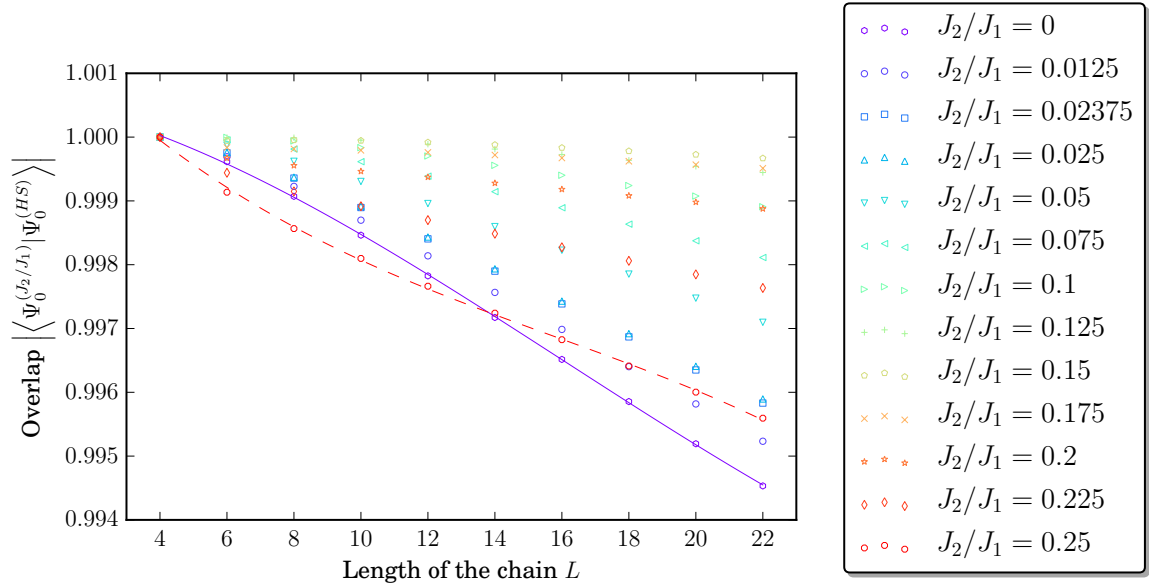


Figure 5.7: Scaling with the length L of the chain of the overlap between ground states of the Haldane-Shastry Hamiltonian \mathcal{H}_{HS} defined in equation 4.20 and the J_2/J_1 Hamiltonian computed via the formula $|\langle \Psi_0^{(J_2/J_1)} | \Psi_0^{HS} \rangle|$ for different J_2/J_1 models. These results were obtained using the analytical solution for $|\Psi_0^{(HS)}\rangle$, i.e. equation 4.22. The purple solid (red dashed) curve is the numerical fitting of the data for $J_2/J_1 = 0$ ($J_2/J_1 = 0.25$) based on the ansatz of equation 5.1.

Furthermore, one can see that there appears an unexpected behaviour for the two cases of interest $J_2/J_1 = 0$ and $J_2/J_1 = 0.25$, that not only they both decay more or less with the same intensity, but they also cross each other at around $L = 14$, as seen by the continuum fitting curves of figure 5.7. In order to visualize these effects more clearly, we plotted the overlaps with respect to the values of the ratios J_2/J_1 used, for fixed lengths, finding the results presented in figure 5.8.

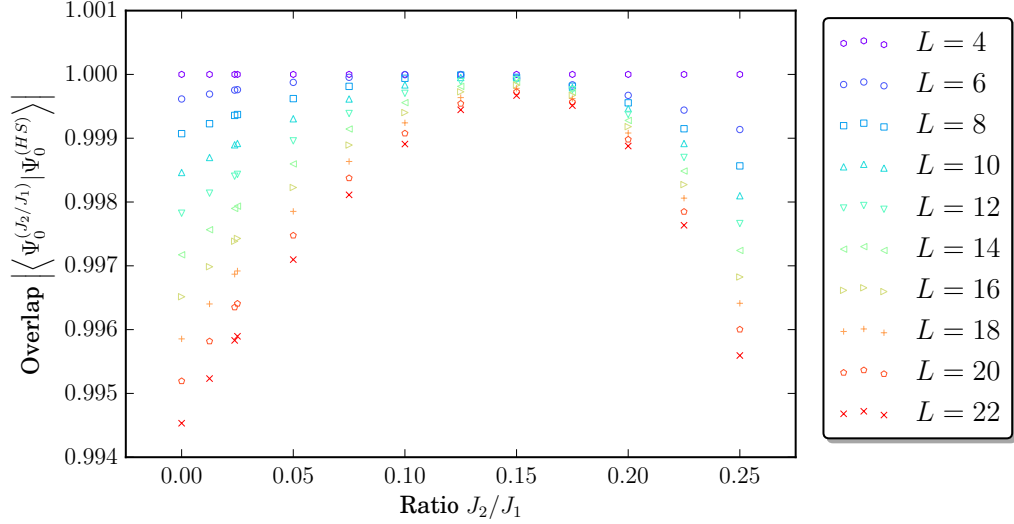


Figure 5.8: Variation with respect to the value of J_2/J_1 for the overlap between ground states of the Haldane-Shastry Hamiltonian \mathcal{H}_{HS} defined in equation 4.20 and the J_2/J_1 Hamiltonian computed via the formula $|\langle \Psi_0^{(J_2/J_1)} | \Psi_0^{HS} \rangle|$ for different J_2/J_1 models. These results were obtained using the analytical solution for $|\Psi_0^{(HS)}\rangle$, i.e. equation 4.22.

The fact that the overlap $|\langle \Psi_0^{(J_2/J_1=0.25)} | \Psi_0^{HS} \rangle|$ does not behave as expected, or at least in the range of lengths L we have been able to probe, could be due to the approximation that led to equation 4.23 not standing true in this regime, making non-negligible the terms of larger interaction (i.e. next-to-next-to-nearest neighbours and so on). As shown by figure 5.8, the overlaps of all lengths used seem to reach very close and highest values for a ratio $J_2/J_1 \approx 0.15$, instead of $J_2/J_1 = 0.25$. However, there is not in principle any reason why this happens, and remains as an open question. Here, it is believed that an intermediate value for the ratio J_2/J_1 lying between 0 and 0.25 could take into account the effects of discarded terms in the expansion of equation 4.23. It would be also of interest to find out whether for a wide range of lengths and J_2/J_1 values any kind of pattern could emerge.

J_2/J_1	0	0.0125	0.02375	0.025	0.05	0.075	0.1	0.125	0.15	0.175	0.2	0.225	0.25
$-e_0$	0.4431	0.4409	0.4388	0.4388	0.4341	0.4300	0.4252	0.4211	0.4167	0.4126	0.4085	0.4045	0.4007
v	1.57	1.54	1.51	1.51	1.46	1.43	1.41	1.31	1.36	1.26	1.21	1.15	1.08
C	0.1114	0.1105	0.1094	0.1094	0.1083	0.1076	0.1062	0.1030	0.0998	0.0960	0.0904	0.08702	0.08335
c'_2	0.5644	0.5659	0.5676	0.5676	0.5692	0.5709	0.5723	0.5736	0.5741	0.5757	0.5774	0.5788	0.5801
f_2	0.1359	0.1364	0.1373	0.1373	0.1386	0.1402	0.1415	0.1455	0.1501	0.1542	0.1585	0.1600	0.1615
c	1.0250	1.0267	1.0267	1.0287	1.0302	1.0319	1.0335	1.0352	1.0370	1.0387	1.0406	1.0426	1.0445
<i>shift</i>	0.7268	0.7268	0.7268	0.7268	0.7268	0.7268	0.7268	0.7268	0.7268	0.7268	0.7268	0.7268	0.7268
a_0	1.0006	1.0005	1.0003	1.0003	1.0001	0.9999	0.9998	0.9998	1.0000	1.0002	1.0006	1.0012	1.0019
$a_1 \times 10^5$	-9.4423	-5.6345	-2.5992	-2.2897	2.9205	5.9680	6.6037	4.5480	-0.5099	-8.9074	-20.9910	-37.0821	-57.3894
$a_2 \times 10^5$	-1.5237	-1.5100	-1.4818	-1.4773	-1.3535	-1.1469	-0.8532	-0.4698	0.0027	0.5577	1.1779	1.8273	2.4373
$a_3 \times 10^7$	3.1693	3.1231	3.0478	3.0363	2.7399	2.2700	1.6189	0.7841	-0.2287	-1.3989	-2.6810	-3.9877	-5.1611

Table 5.1: Numerical values obtained after fitting the data computed via exact diagonalization of the pertinent Hamiltonians. The parameters appearing in different parts of this work are separated by horizontal lines. Thus, parameters $\{e_0, L\}$ appear in equation 4.4 for the case of the ground state energy per site $E_0(L)/L$, C in equation 4.8 for the value of the correlator between two spins at positions 0 and r , $\{c'_2, f_2\}$ in equation 4.19 for the value of the 2-Rényi entropies $S^{(2)}(l)$ for a subchain of length l , c in equation 4.12 for the value of the Von Neumann entropies $S(l)$ for a subchain of length l , and finally parameters $\{a, b, c, d\}$ in equation 5.1 for the value of the overlaps between the ground states of \mathcal{H}_{J_2/J_1} and \mathcal{H}_{HS} . The parameter *shift* is just a constant added to the Von Neumann entropy case to fit the data points better.

6

Conclusions and Outlook

In this work, a numerical method based on exact diagonalization has been developed from the beginning using first principles, allowing us to study Hamiltonian lattices relevant in the Condensed Matter Physics area. This, permitted to form a connection with the world of High Energy Physics passing through the foundations of Quantum Field Theory. Besides, the numerical simulations of these systems are of experimental interest, since they allow researchers to understand better how possible physical realizations of these models could be performed. This is nowadays a rapid developing field, concerning e.g. the experimental confirmation of the results obtained throughout this work using quantum macroscopic systems as optical laser lattices.

Being able to probe the realm of quantum many-body physical systems such as spin chains models, which is a rather fascinating and valuable outcome in itself, has provided results with which confirmation of those obtained in 1989 by Affleck *et al.* was possible. Hence, it has been verified that indeed the continuum limit of the well-known and widely studied Heisenberg Hamiltonian is the $SU(2)_{k=1}$ Wess-Zumino-Witten non-linear σ -model, which has a direct correspondence with Conformal Field Theory with central charge $c = 1$. This confirmation made reasonable to extend the study to a whole class (the J_2/J_1 models) and discuss in which cases a valid description by a CFT still holds and what the effects of moving away from the critical points are. Furthermore, the relation amongst the models studied here and Haldane-Shastry's one, has been explored, finding unexpected results that waits still for an explanation and further study.

From the basic results, as the visualization of the conformal towers and the scaling of the ground state energy are, one can proceed to study correlations of operators and entanglement entropies in order to understand better how the distinct parts conforming a spin chain talk to each other. This path showed to be very fruitful in this work, allowing a connection of, *a priori* well-known Physics, as spin chain models, with one more recent, as Quantum Information ideas are, what seem to be an important field of research in the coming years.

Some of the possible ways this work could be extended would be improving the numerical algorithms, in order to reach larger sizes and thus probe corrections predicted by the theory that here was not possible to study. Particular methods of doing so would be adding reflection (parity) and inversion symmetries in the construction of the Hamiltonian matrix. It would also be interesting to study the advantages of the numerical methods used in this work with respect to others also well-established as DMRG or quantum Monte-Carlo algorithms. In particular, this comparison could be done when studying the entanglement entropies of not only the ground state but excited ones too, since there are analytical formulae and predictions that come from Quantum Information ideas.

Bibliography

- [1] K. Joël, D. Kollmar, and L. F. Santos, “An introduction to the spectrum, symmetries, and dynamics of spin-1/2 Heisenberg chains”, *Am. J. Phys.* **81**, 450 (2013).
- [2] I. Chigak and H. Mukaida, “Non-abelian gauge theory for quantum Heisenberg antiferromagnetic chain”, *J. Phys. A: Gen. Phys.* **27**, 4695–4708 (1994).
- [3] H. Bethe, “Zür theorie der metalle. I. Eigenwerte und Eigenfunktionen der linearen Atomkette”, *Z. Phy.*, 205 (1931).
- [4] A. O. Gogolin, A. A. Nersesyan, and A. M. Tsvelik, *Bosonization and strongly correlated systems* (Cambridge University Press, 1999).
- [5] A. M. Tsvelik, *Quantum field theory in condensed matter physics*, Second (Cambridge University Press, 2003).
- [6] P. Jordan and E. Wigner, “The collected works of eugene paul wigner”, in , edited by A. Wightmann (Springer-Verlag Berlin Heidelberg, 1993) Chap. Über das Paulische Äquivalenzverbot. Pp. 109–129.
- [7] C. Itoi and H. Mukaida, “Non-abelian gauge theory for quantum heisenberg antiferromagnetic chain”, *J. Phys. A: Math. Gen.* **27**, 4695–4708 (1994).
- [8] F. D. M. Haldane, “Nonlinear field theory of large-spin Heisenberg antiferromagnets: semiclassically quantized solitons of the one-dimensional easy-axis Néel state”, *Phys. Rev. Lett.* **50**, 1153 (1983).
- [9] I. Affleck and F. D. M. Haldane, “Critical theory of quantum spin chains”, *Phys. Rev. B* **36**, 5291–5300 (1987).

- [10] F. D. M. Haldane, “O(3) Non-linear model and the topological distinction between integer- and half-integer-spin antiferromagnets in two dimensions”, *Phys. Rev. Lett.* **61**, 1029–1032 (1988).
- [11] I. Affleck, “Quantum spin chains and the Haldane gap”, *J. Phys.: Condens. Matter.* **1**, 3047–3072 (1989).
- [12] A. A. Belavin, A. M. Polyakov, and A. B. Zamolodchikov, “Infinite conformal symmetry in two-dimensional quantum field theory”, *Nucl. Phys. B* **241**, 333–380 (1984).
- [13] J. Cardy, “Conformal invariance and universality in finite-size scaling”, *J. Phys. A: Gen. Phys.* **17**, L385–L387 (1984).
- [14] J. Cardy, “Finite-size scaling in strips: antiperiodic boundary conditions”, *J. Phys. A: Gen. Phys.* **17**, L961–L964 (1984).
- [15] H. Blöte, J. Cardy, and M. Nightingale, “Conformal invariance, the central charge, and universal finite-size amplitude at criticality”, *Phys. Rev. Lett.* **56**, 742–745 (1986).
- [16] V. Dotsenko and V. Fateev, “Conformal algebra and multipoint correlation functions in 2d statistical models”, *Nucl. Phys. B* **240** (1984) [10.1016/0550-3213\(84\)90269-4](https://doi.org/10.1016/0550-3213(84)90269-4).
- [17] I. Affleck, D. Gepner, H. J. Schulz, and T. Ziman, “Critical behaviour of spin-s Heisenberg antiferromagnetic chains: analytic and numerical results”, *J. Phys. A: Math. Gen.* **22**, 511–529 (1989).
- [18] C. Holzhey, F. Larse, and F. Wilczek, “Geometric and renormalized entropy in conformal field theory”, *Nucl. Phys. B* **424**, 443–467 (1994).
- [19] G. Vidal, J. Latorre, E. Rico, and A. Kitaev, “Entanglement in quantum critical phenomena”, *Phys. Rev. Lett.* **90** (2003) [10.1103/PhysRevLett.90.227902](https://doi.org/10.1103/PhysRevLett.90.227902).
- [20] P. Calabrese and J. Cardy, “Entanglement entropy and quantum field theory”, *J. Stat. Mech: Theory Exp.* **P10020+** (2004) [10.1088/1742-5468/2004/06/P06002](https://doi.org/10.1088/1742-5468/2004/06/P06002).
- [21] P. Calabrese and J. Cardy, “Evolution of entanglement entropy in one–dimensional systems”, *J. Stat. Mech.* **0504 P04010** (2005) [10.1088/1742-5468/2005/04/P04010](https://doi.org/10.1088/1742-5468/2005/04/P04010).
- [22] P. Calabrese, M. Campostrini, F. Essler, and B. Nienhuis, “Parity effects in the scaling of block entanglement in gapless spin chains”, version 2, *Phys. Rev. Lett.* **104** (2010) [10.1103/PhysRevLett.104.095701](https://doi.org/10.1103/PhysRevLett.104.095701).

- [23] F. Castilho Alcaraz, M. Ibáñez Berganza, and G. Sierra, “Entanglement of low-energy excitations in conformal field theory”, version 2, *Phys. Rev. Lett.* **106** (2011) 10.1103/PhysRevLett.106.201601.
- [24] H. Nishimori, “Titpack - Numerical diagonalization routines and quantum spin hamiltonians”, in *AIP Conference Proceedings*, Vol. 248 (1992), p. 269.
- [25] S. R. White, “Density matrix formulation for quantum renormalization groups”, *Phys. Rev. Lett.* **69**, 2863–2866 (1992).
- [26] S. R. White, “Density-matrix algorithms for quantum renormalization groups”, *Phys. Rev. B* **48**, 10345 (1993).
- [27] F. D. M. Haldane, “Exact jastrow-gutzwiller resonating-valence-bond ground state of the spin-1/2 antiferromagnetic Heisenberg chain with $1/r^2$ exchange”, *Phys. Rev. Lett.* **60**, 635–638 (1988).
- [28] B. S. Shastry, “Exact solution of an $S = \frac{1}{2}$ Heisenberg antiferromagnetic chain with long-ranged interactions”, *Phys. Rev. Lett.* **60**, 639–642 (1988).
- [29] J. A. Hoyos, A. P. Vieira, N. Laflorencie, and E. Miranda, “Correlation amplitude and entanglement entropy in random spin chains”, version 2, *Phys. Rev. B* **76**, 174425 (2007).
- [30] J. Richter, R. Zinke, and D. Farnell, “The spin-1/2 square-lattice $J_1 - J_2$ model: the spin-gap issue”, *Eur. Phys. J. B* **88** (2015) 10.1140/epjb/e2014-50589-x.
- [31] C. Yang and C. P. Yang, “One dimensional chain of anisotropic spin-spin interactions. i. proof of Bethe’s hypothesis for ground state in a finite system”, *Phys. Rev.* **150**, 321 (1966).
- [32] C. Yang and C. Yang, “One-dimensional chain of anisotropic spin-spin interactions. II. properties of the ground-state energy per lattice site for an infinite system”, *Phys. Rev.* **150**, 327 (1966).
- [33] C. Yang and C. Yang, “One-dimensional chain of anisotropic spin-spin interactions. III. applications”, *Phys. Rev.* **151**, 258 (1966).
- [34] I. Affleck, “Field theory methods and quantum critical phenomena”, in *Les Houches 1988, session XLIX, Fields, Strings and Critical Phenomena*, edited by E. Brézin and J. Zinn-Justin (1988).
- [35] V. Knizhnik and A. B. Zamolodchikov, “Current algebra and Wess-Zumino model in two dimensions”, *Nucl. Phys. B* **247**, 83–103 (1984).

- [36] P. Di Francesco, P. Mathieu, and D. Sénéchal, *Conformal field theory* (Springer, 1997).
- [37] R. Chitra, S. Pati, H. R. Krishnamurthy, D. Sen, and S. Ramasesha, “Density-matrix renormalization-group studies of the spin-half Heisenberg system with dimerization and frustration”, version 2, *Phys. Rev. B* **52**, 6581–6587 (1995).
- [38] F. Verstraete and J. I. Cirac, “Renormalization algorithms for quantum-many body systems in two and higher dimensions”, arXiv preprint cond-mat/0407066 (2004).
- [39] J. I. Cirac and F. Verstraete, “Renormalization and tensor product states in spin chains and lattices”, *J. Phys. A: Math. Theor.* **42** (2009) [10.1088/1751-8113/42/50/504004](https://doi.org/10.1088/1751-8113/42/50/504004).
- [40] R. Orus, “A practical introduction to tensor networks: Matrix product states and projected entangled pair states”, *Ann. Phys.* **349**, 117–158 (2014).
- [41] A. W. Sandvik, “Computational studies of quantum spin systems”, in *Lectures on the Physics of Strongly Correlated Systems XIV*, Vol. 1297, edited by A. A. Ā. Mancini (2010), pp. 135–338.
- [42] R. Lehoucq, D. Sorensen, and C. Yang, *ARPACK USERS GUIDE: solution of large scale eigenvalue problems by implicitly restarted arnoldi methods*. (SIAM, Philadelphia, PA, 1998).
- [43] K. Hallberg, P. Horsch, and G. Martinez, “Numerical renormalization group study of the correlation functions of the antiferromagnetic spin- $\frac{1}{2}$ Heisenberg chain”, *Phys. Rev. B* **52** (1995) [10.1103/PhysRevB.52.R719](https://doi.org/10.1103/PhysRevB.52.R719).
- [44] T. Kaplan, P. Horsch, and J. Borysowicz, “Finite-size scaling in the ground state of spin-1/2 antiferromagnetic XXZ rings”, *Phys. Rev. B* **35**, 1877 (1987).
- [45] H. Q. Lin and D. K. Campbell, “Spin-spin correlations in the one-dimensional spin- $\frac{1}{2}$ antiferromagnetic heisenberg chain”, *J. Appl. Phys.* **69**, 5947 (1991).
- [46] J. I. Cirac and G. Sierra, “Infinite matrix product states, conformal field theory, and the Haldane-Shastry model”, *Phys. Rev. B* **81** (2010) [10.1103/PhysRevB.81.104431](https://doi.org/10.1103/PhysRevB.81.104431).
- [47] A. E. Nielsen, J. I. Cirac, and G. Sierra, “Quantum spin hamiltonians for the $SU(2)_k WZW$ model”, version 2, *J. Stat. Mech.* **P11014** (2011) [10.1088/1742-5468/2011/11/P11014](https://doi.org/10.1088/1742-5468/2011/11/P11014).



Representation theory and CFT explained in detail

Mostly of this section is a brief summary of concepts needed to keep the coherence in this work at an understandable level without rising its extension too much. For the formal reader, we would suggest to consult the many concepts included here in the excellent standard book by Di Francesco *et al.* of reference [36].

A.1 Why CFT's are relevant?

In general, in Physics, we are interested in theories that describe the behaviour of some fields of interest. These theories may contain symmetries, which are powerful allies as the great scientist Emmy Noether proved in her famous theorem. A symmetry appears whenever a specific type of transformation of our fields leaves the Lagrangian of our theory invariant. A particular kind of these transformations are *scale transformations*, which for a field ϕ are defined as:

$$\tilde{\phi}(x) = s^\xi \phi(sx), \tag{A.1}$$

with s being the *dilation factor*, and ξ the *scaling dimension* of the field ϕ .

For a given action $\mathcal{S}[\phi]$ for the field ϕ , we assume there exists a *fixed-point action* $\mathcal{S}_0[\phi]$ at some point in parameter space. In the neighbourhood of this point we can

write:

$$\mathcal{S}[\phi] = \mathcal{S}_0[\phi] + \sum_i u_i \int dx \hat{O}_i(x), \quad (\text{A.2})$$

with $\hat{O}_i(x)$ being local operators, and u_i the couplings of these operators, which must be small if we are close to the fixed point.

Thus, under renormalization-group (scale) transformations

$$\tilde{\mathcal{S}}[\phi] = \mathcal{S}_0[\phi] + \sum_i \tilde{u}_i(s) \int dx \hat{O}_i(x), \quad (\text{A.3})$$

and hence $\tilde{\hat{O}}_i(x) = s^{\xi_i} \hat{O}_i(sx)$, which leads to

$$\tilde{u}_i = u_i s^{d-\xi_i}. \quad (\text{A.4})$$

This equation tells us how the couplings of each of the local operators appearing in the expansion of the action in the neighbourhood of its fixed point vary under renormalization-group (scale) transformations. We can differentiate several possible behaviours for the couplings depending of the value of the scaling dimension with respect to the actual dimension d :

relevant: grow under renormalization: $\xi_i < d$,

irrelevant: vanish under renormalization: $\xi_i > d$,

marginal: stay constant or vary logarithmically under renormalization: $\xi_i = d$.

These definitions are of significant importance, since they give terminology to speak about the behaviour of the theories near critical points and how, when considering renormalization flows, new operators and terms appear in correlators. It is important to keep in mind that the nature of the scaling of the couplings depends not only on the form of these operators in terms of ϕ , but also on the fixed point considered, which in our case was taken to be without loss of generality as the origin.

Fixed points under renormalization are invariant under *scalings*, i.e. zooming in/out. This particular type of transformations belong to a more general class that defines a *Conformal Field Theory* (CFT).

A.2 Transformations in a CFT and algebras of their generators

A CFT has *conformal transformations*, which preserve angles between vectors:

$$g_{\mu\nu} \rightarrow \tilde{g}_{\rho\sigma} = \Delta(x)g_{\mu\nu}, \quad (\text{A.5})$$

where $\Delta(x) > 0$ is a local rescaling. Generally, conformal transformations are generally formed by the full Poincaré group (translations, rotations, boosts) which has $\Delta = 1$ and scalings and special conformal transformations. A generic transformation of the metric $g(x)$ at point x can be written in terms of the coordinates as

$$\tilde{g}_{\rho\sigma}(x') = \frac{\partial x'^{\rho}}{\partial x^{\mu}} \frac{\partial x'^{\sigma}}{\partial x^{\nu}} g_{\mu\nu}(x). \quad (\text{A.6})$$

This expression gives a coordinate-dependent expression for the rescaling parameter $\Delta(x)$. If one considers a generic mapping

$$x'^{\rho} = x^{\rho} + \epsilon^{\rho}(x) + \mathcal{O}(\epsilon^2), \quad (\text{A.7})$$

infinitesimally close to the identity ($\epsilon^{\rho}(x) \approx 0$), and substitutes into equation A.6 one finds that, after expanding $\Delta(x)$ to first order in ϵ , conformal means

$$\partial_{\mu}\epsilon_{\nu} + \partial_{\nu}\epsilon_{\mu} = \kappa(x)\eta_{\mu\nu}, \quad (\text{A.8})$$

where $\eta_{\mu\nu}$ is the Minkowski metric and

$$\kappa(x) = \frac{2}{d}\partial_{\mu}\epsilon^{\mu} = 0, \quad (\text{A.9})$$

and d is the dimension of our space-time. Using both last two equations, who are called *conformal Killing equations* (CKE) in the literature, one can prove that

$$(d-1)\partial_{\nu}\partial^{\nu}(\partial_{\mu}\epsilon^{\mu}) = 0. \quad (\text{A.10})$$

In the particular case that concerns us the most ($d = 1 + 1 = 2$) something very remarkable happens. Switching momentarily to Euclidean (namely $\epsilon = \begin{pmatrix} \epsilon_0 \\ \epsilon_1 \end{pmatrix}$) lets us see that the conformal equations A.8, A.9, and A.10, are simply Cauchy-Riemann

equations:

$$\partial_0 \epsilon_0 - \partial_1 \epsilon_1 = 0, \quad (\text{A.11})$$

$$\partial_1 \epsilon_0 + \partial_0 \epsilon_1 = 0, \quad (\text{A.12})$$

so conformal transformations in $d = 2$ are just *holomorphic* ($\partial_{\bar{z}} \epsilon = 0$ with $\epsilon = x_0 + ix_1$) transformations, which are analytic over the hole space.

Belavin, Polyakov, and Zamolodchikov [12], realised that this two-dimensional group could be enhanced into an infinite-dimensional one, turning holomorphic into *meromorphic*, i.e. holomorphic in an open set of the complex plane, allowing it to have divergences (poles) so they admit a Laurent expansion: $\epsilon(z) = \sum_{n \in \mathbb{Z}} \epsilon_n (-z^{n+1})$. The generators $\{l_n, \bar{l}_n\}$ associated to this transformations satisfy a *Witt algebra*:

$$[l_n, l_m] = (m - n)l_{m+n}, \quad (\text{A.13})$$

$$[l_n, \bar{l}_m] = 0 \quad (\text{A.14})$$

and similarly for \bar{l} . This algebra is the *local conformal algebra*, since not all transformations generated are invertible. It contains the *global conformal algebra*, generated by a subset of these generators $\{l_{-1}, l_0, l_{+1}\}$. Note how the generators map into the conformal transformations (and similarly for \bar{l}):

complex translations: $l_{-1} = -\partial_z$,

scalings and rotations: $l_0 = -z\partial_z$,

special conformal transformations: $l_{+1} = -z^2\partial_z$.

We are now in position of defining the *Virasoro algebra*, which is the *central extension* of the Witt algebra. This means that we add some extra generators to the algebra, doing a direct sum with a complex, being this complex element represented by the *central charge* c , and the Virasoro algebra is defined:

$$[L_m, L_n] = (m - n)L_{m+n} + \frac{c}{12}m(m^2 - 1)\delta_{m+n,0}, \quad (\text{A.15})$$

where the generators $\{L_m\}$ refer only to the subset of global conformal generators, i.e. $\{l_m\}$ with $m = \{-1, 0, +1\}$. This algebra satisfies the requirements to be a *Lie algebra*.

In general, a Lie algebra \mathfrak{g} with generators J^a is a vector space equipped with an anti-symmetric binary operation $[\cdot, \cdot]$, called a commutator, mapping $\mathfrak{g} \times \mathfrak{g}$ into

\mathfrak{g} , and further constrained to satisfy the Jacobi identity

$$[[X, [Y, Z]] + [Z, [X, Y]] + [Y, [Z, X]] = 0 \quad \text{for } X, Y, Z \in \mathfrak{g}. \quad (\text{A.16})$$

We can construct a generalization of a Lie algebra \mathfrak{g} in which we admit that the generators $\{J^a\}$ are also Laurent polynomials in some variable z . The set of such polynomials is denoted by $\mathbb{C}[z, z^{-1}]$. This generalization is called the *loop algebra* $\tilde{\mathfrak{g}}$:

$$\tilde{\mathfrak{g}} = \mathfrak{g} \otimes \mathbb{C}[z, z^{-1}], \quad (\text{A.17})$$

with generators $\{J_n^a\}$ defined as $J^a \otimes z^n$. The algebra multiplication rule extends naturally from \mathfrak{g} to $\tilde{\mathfrak{g}}$ as

$$[J_n^a, J_m^b] = \sum_c i f_c^{ab} J_{n+m}^c. \quad (\text{A.18})$$

We can still do a central extension $\tilde{\mathfrak{g}} \oplus \mathbb{C}\hat{k}$ as follows:

$$[J_n^a, J_m^b] = \sum_c i f_c^{ab} J_{n+m}^c + \hat{k} n \delta_{ab} \delta_{n+m,0}, \quad (\text{A.19})$$

where we took that $[J_n^a, \hat{k}] = 0$ and that the generators J^a of \mathfrak{g} are orthonormal with respect to the *Killing form*, which for two generators J^a and J^b is defined as $\text{Tr}(\text{ad} J^a \text{ad} J^b)$, with $\text{ad}(J^a)J^b \equiv [J^a, J^b]$ being the *adjoint representation*. From the algebra of equation A.19, we can again do another central extension with the addition of the operator L_0 (corresponding to the previous l_0 defined in terms of z when speaking about scalings and rotations) to obtain an *affine* Lie algebra $\hat{\mathfrak{g}}$:

$$\hat{\mathfrak{g}} = \tilde{\mathfrak{g}} \oplus \mathbb{C}\hat{k} \oplus \mathbb{C}L_0. \quad (\text{A.20})$$

This extension is done in order to have all the generators of the maximal *Cartan subalgebra*, which is the algebra made up by the set of all commuting hermitian operators [36]. It is the expression of equation A.20 that precisely defines what a *Kac-Moody algebra* is. It is clearly an infinite dimensional algebra, given that it has an infinite number of generators $\{J_n^a\}$, with $n \in \mathbb{Z}$.

A.3 Quantum field theories with conformal invariance in a two dimensional theory

Now that the transformations present in our theory are correctly defined, we can act with them on our fields. Our goal is to find what the implications of conformal

invariance in a quantum field theory are. Our fields will be functions of the space-time coordinates (x^0, x^1) , that can be written as functions of the conformal ones (z, \bar{z}) by

$$x^0 = \frac{1}{2}(z + \bar{z}), \quad (\text{A.21})$$

$$x^1 = \frac{1}{2i}(z - \bar{z}). \quad (\text{A.22})$$

Note that in principle, \bar{z} is different from the conjugated of z , z^* . However, from all possible transformations generated from the generators studied in the previous part of this section, only the physical ones will be of interest. Two important examples of this will be the time translations generated by the Hamiltonian, $\mathcal{H} = L_0 + \bar{L}_0$, and the spatial translations, generated by the momentum operator, $\mathcal{P} = i(L_0 - \bar{L}_0)$. Using these physical operators guarantees that the physical surface $z^* \equiv \bar{z}$ will be conserved. This will be taken for granted hereinafter, since only physical operators are of interest.

We can classify our fields using their dependence on their variables, saying that a field $\phi(z, \bar{z})$ is *chiral/holomorphic/left (anti-chiral/anti-holomorphic/right)* if it contains only dependence on z (\bar{z}).

Another possible classification is based on looking at the way the fields transform under a generic mapping $z \rightarrow f(z)$ (which will be eventually related to the initial discussion around equation A.1 and scale transformations):

$$\phi(z, \bar{z}) \rightarrow \tilde{\phi}(z, \bar{z}) = \left(\frac{\partial f}{\partial z}\right)^h \left(\frac{\partial \bar{f}}{\partial \bar{z}}\right)^{\bar{h}} \phi(f(z), \bar{f}(\bar{z})), \quad (\text{A.23})$$

where the *conformal weights* of the field ϕ are defined as

$$(h, \bar{h}) = \frac{1}{2}(\xi + s, \xi - s) \quad (\text{A.24})$$

and ξ and s are respectively the scaling dimension and the spin of the field ϕ . Note that $\bar{h} \neq h^*$. The conformal weights h (\bar{h}) and are also called *(anti-)holomorphic conformal dimensions*.

If equation A.23 is fulfilled by all the global conformal transformations, generated by the Virasoro algebra of equation A.15, we say the field is a *primary field*. If, instead, we need the full local conformal algebra, we say the field is a *quasi-primary field*. It is easy to see hence that all primary fields are quasi-primary, while the reverse is not true in general.

Under an infinitesimal transformation $x^\mu \rightarrow x^\mu + \epsilon^\mu(x)$, a primary field transforms as

$$\phi(z, \bar{z}) \rightarrow \phi(z, \bar{z}) + (h\partial_z \epsilon + \epsilon \partial_z) \phi(z, \bar{z}) + \text{a.c.}, \quad (\text{A.25})$$

with a.c. standing for anti-chiral. Thus, the variation of the field can be written as

$$\delta_{\epsilon, \bar{\epsilon}} \phi(z, \bar{z}) = (h\partial_z \epsilon + \epsilon \partial_z + \text{a.c.}) \phi(z, \bar{z}). \quad (\text{A.26})$$

One field whose variation has exactly this form, i.e. it is a quasi-primary field, is the *energy-momentum tensor* $T_{\mu\nu}$ itself, which can be understood as the response of the theory to changes in the metric $g_{\mu\nu} \rightarrow g_{\mu\nu} + \delta g_{\mu\nu}$. This is related to the conservation of a quantity, via the Noether's theorem. What is conserved due to conformal symmetries? Take the following ansatz for a conserved current j_μ :

$$j_\mu = T_{\mu\nu} \epsilon^\nu. \quad (\text{A.27})$$

If ϵ^ν is due to a conformal transformation, using that the current j^μ must have null divergence we arrive to

$$\partial^\mu T_{\mu\nu} = 0. \quad (\text{A.28})$$

It can be proven that the CKE's A.8 and A.9, together with the fact that the current j_μ is conserved, imply that

$$\partial^\mu j_\mu = \frac{1}{2} T_{\mu\nu} (\partial_\rho \epsilon^\rho \eta^{\mu\nu}) = 0, \quad (\text{A.29})$$

and hence

$$T_\mu^\mu = 0 \quad (\text{A.30})$$

must be true for any CFT. Note that the case $d = 2$ was already taken, otherwise a factor $2/d$ would appear in equation A.29 multiplying the parenthesis. Thus, one finds that the energy-momentum tensor expressed in the conformal coordinates (z, \bar{z}) , defined by the inverse to the equations A.21 and A.22, satisfies

$$\partial_z T_{\bar{z}\bar{z}} = 0, \quad (\text{A.31})$$

$$\partial_{\bar{z}} T_{zz} = 0. \quad (\text{A.32})$$

This means that the tensor T can be decomposed into chiral and anti-chiral components:

$$T = \begin{pmatrix} T(z) & 0 \\ 0 & \bar{T}(\bar{z}) \end{pmatrix} = \begin{pmatrix} \frac{1}{2}(T_{00} - iT_{10}) & 0 \\ 0 & \frac{1}{2}(T_{00} + iT_{10}) \end{pmatrix}. \quad (\text{A.33})$$

Using this energy-momentum tensor and the current of equation A.27 we can finally find the conserved charge $Q_{\epsilon, \bar{\epsilon}}$ used in quantum field theories to compute the *Ward identities* ($\delta_{\epsilon, \bar{\epsilon}}\phi = -[Q_{\epsilon, \bar{\epsilon}}, \phi]$):

$$Q_{\epsilon, \bar{\epsilon}} = \frac{1}{2\pi i} \oint_{\mathcal{C}} [dz\epsilon(z)T(z) + \text{a.c.}] \quad (\text{A.34})$$

with $Q = \int dx^1 j_0$ as usually. The integral is defined over a circuit evaluated at equal time x^1 . This is done via the process called *radial quantization*, in which we define the CFT over a cylinder with different times meaning different sections perpendicular to the axis of revolution of the cylinder. This quantization procedure allows us to *radial order* the operators via the radial-ordering operator $\mathcal{R}(\cdot)$ to find that the Ward identity derived from the charge of equation A.34 is

$$\delta_{\epsilon, \bar{\epsilon}}\phi(w, \bar{w}) = \oint_{\mathcal{C}(w)} dz\epsilon(z)\mathcal{R}(T(z)\phi(w)) + \text{a.c.} \quad (\text{A.35})$$

with $\mathcal{C}(w)$ being a circuit encircling the point w and with

$$\mathcal{R}(T(z)\phi(w, \bar{w})) = \frac{h}{(z-w)^2}\phi(w, \bar{w}) + \frac{1}{z-w}\partial_w\phi(w, \bar{w}) + \text{non-singular terms.} \quad (\text{A.36})$$

Equation A.36 (and similarly its anti-chiral counterpart) defines what the *operator product expansion* (OPE) of a field is. The OPE's allow us to compute correlation functions. For instance, it can be proven that

$$T(z)T(w) = \frac{c/2}{(z-w)^4} + 2\frac{T(w)}{(z-w)^2} + \frac{\partial_w T(w)}{z-w}. \quad (\text{A.37})$$

Notice that the term proportional to the central charge c is a non-primary contribution, spoiling the primary character of the energy-momentum tensor. This is precisely the reason behind referring to c as the *conformal anomaly parameter*. Notice that if $c = 0$ the energy-momentum tensor would be a primary field with conformal weight $h = 2$. The central charge term can be seen to describe the short-distance behaviour of the theory, being the cause of imposing a scale in our system.

In order to do a consistency check of equation A.37 one could remember that the job of $T(z)$ was generating the conformal transformations. The generators of the global conformal group were the Virasoro generators fulfilling equation A.15, so they cannot be independent of the energy-momentum tensor. In fact, the Virasoro generators are the Laurent modes of the energy-momentum tensor:

$$T(z) = \sum_{n \in \mathbb{Z}} L_n z^{-n-2}. \quad (\text{A.38})$$

Having done this correspondence, we can now proceed to mention some important remarks about representation theory of *minimal models*.

A.4 Minimal models and highest-weight representation

In a CFT we expect the energy eigenstates (i.e. eigenstates of $L_0 + \bar{L}_0$) to fall within representations of the global conformal algebra (the Virasoro algebra) much in the same way as the energy eigenstates of a rotations-invariant system fall into irreducible representations of $\mathfrak{su}(2)$.

As in the theory of angular momentum, we use a *highest-weight representation* choosing a single generator, L_0 , since no pair of generators commute in the Virasoro algebra of equation A.15. This construction, also called a *Verma module*, will be diagonal in the representation space. We will denote it by $\mathcal{V}(c, h)$, with c the central charge, and h the eigenvalue of the highest-weight state $|h\rangle$, namely

$$L_0|h\rangle = h|h\rangle, \quad (\text{A.39})$$

and $|h\rangle$ being the asymptotic state created by applying a primary field operator $\phi(0)$ of dimension h on the vacuum $|0\rangle$. These states fulfil that $L_n|h\rangle = 0$ for $n > 0$, reason for which we say that the generators $\{L_{n>0}\}$ are *raising operators*. The states obtained by applying the *lowering operators* $\{L_{n<0}\}$ on $|h\rangle$ are called *descendant states* for obvious reasons, and they form the so-called *conformal towers*, being each row of the tower (of *a priori* different width) called the *level of the descendant*.

In general, the Hilbert space is a direct sum of tensor products of the Verma modules over all conformal dimensions of the theory:

$$\sum_{h, \bar{h}} \mathcal{V}(c, h) \otimes \bar{\mathcal{V}}(c, \bar{h}). \quad (\text{A.40})$$

If the number of Verma moduli $\mathcal{V}(c, h)$ is finite, it means that the *holomorphic characters* follow a particular transformation law under a given *modular transformation*. This allows to reorganize an in principle infinite number of primary fields into a finite number of blocks. This would correspond to a *extended symmetry algebra*, and the CFT's that satisfy this are called *rational conformal field theories* (RCFT's) [36].

It may happen that a descendant state $|\chi\rangle$ in a Verma module $\mathcal{V}(c, h)$ would also be a primary state of $h_\chi > h$, decoupling from the other fields. If this happens, the operator algebra changes and presents a particular structure, and we call the state $|\chi\rangle$ a *null state*. This has been used [47] to develop, via the characters of the moduli, an easy procedure to construct quantum Hamiltonians for RCFT's with $SU(2)_k$ Kac-Moody algebras.

The case of highest interest to us in this work is $k = 1$, for which the Kac-Moody algebra defined in equation A.20 can be written in terms of the Laurent modes (see equation A.38) of the energy-momentum tensor of the theory (see equation 2.15), which happen to be the currents of the field theory:

$$[J_n^a, J_m^b] = i \sum_c \epsilon_{abc} J_{n+m}^c + \frac{k}{2} n \delta_{ab} \delta_{n+m,0}, \quad (\text{A.41})$$

where J_n^a are the modes in a Laurent expansion of the $J^a(z)$ chiral left (L) or right (R) currents, namely

$$J^a(z) = \sum_{-\infty}^{+\infty} J_n^a z^{-n+1}. \quad (\text{A.42})$$

Note how the typical $SU(2)$ structure constants of the algebra appear in the first term of equation A.41. The zero modes of the currents, J_0^a , form a closed $SU(2)$ algebra, which in the standard spin basis is given by the following commutation relations:

$$[J_n^0, J_m^0] = \frac{k}{2} n \delta_{n+m,0}, \quad (\text{A.43})$$

$$[J_n^0, J_m^\pm] = \pm J_{n+m}^\pm, \quad (\text{A.44})$$

$$[J_n^+, J_m^-] = 2J_{n+m}^0 + kn \delta_{n+m,0}. \quad (\text{A.45})$$

To construct a valid unitary representation theory of this Kac-Moody algebra,

one associates a primary state $|\phi_j\rangle$ to each of these primary fields, satisfying

$$|\phi_j\rangle = \phi_j(0)|0\rangle, \tag{A.46}$$

$$J_0^a |\phi_j\rangle = t^a |\phi_j\rangle, \tag{A.47}$$

$$J_n^a |\phi_j\rangle = 0 \quad \text{for } n > 0, \tag{A.48}$$

where the t^a are the $2j+1$ -dimensional matrices of the j -spin representation of the $SU(2)$ group. These are precisely the conditions required to construct a highest-weight representation of the algebra, as explained in the beginning of this subsection.



Programs used and codes

Due to the long extension of the written programs used in this work in order to compute numerically the different quantities appearing throughout this dissertation, the author has decided to omit them and not include them here.

However, due to its importance as well as to its original value, the author will be more than eager to send the codes developed to any one who is interested.

To do so, please contact him using the following e-mail direction:

hector.bermudezcastro@gmail.com.